
A Consistent and Differentiable L_p Canonical Calibration Error Estimator

Teodora Popordanoska*
ESAT-PSI, KU Leuven
teodora.popordanoska@kuleuven.be

Raphael Sayer*[†]
University of Tübingen
raphael.sayer@uni-tuebingen.de

Matthew B. Blaschko
ESAT-PSI, KU Leuven
matthew.blaschko@esat.kuleuven.be

Abstract

Calibrated probabilistic classifiers are models whose predicted probabilities can directly be interpreted as uncertainty estimates. It has been shown recently that deep neural networks are poorly calibrated and tend to output overconfident predictions. As a remedy, we propose a low-bias, trainable calibration error estimator based on Dirichlet kernel density estimates, which asymptotically converges to the true L_p calibration error. This novel estimator enables us to tackle the strongest notion of multiclass calibration, called canonical (or distribution) calibration, while other common calibration methods are tractable only for top-label and marginal calibration. The computational complexity of our estimator is $\mathcal{O}(n^2)$, the convergence rate is $\mathcal{O}(n^{-1/2})$, and it is unbiased up to $\mathcal{O}(n^{-2})$, achieved by a geometric series debiasing scheme. In practice, this means that the estimator can be applied to small subsets of data, enabling efficient estimation and mini-batch updates. The proposed method has a natural choice of kernel, and can be used to generate consistent estimates of other quantities based on conditional expectation, such as the sharpness of a probabilistic classifier. Empirical results validate the correctness of our estimator, and demonstrate its utility in canonical calibration error estimation and calibration error regularized risk minimization.

1 Introduction

Deep neural networks have shown tremendous success in classification tasks, being regularly the best performing models in terms of accuracy. However, they are also known to make overconfident predictions [Guo et al., 2017], which is particularly problematic in safety-critical applications, such as medical diagnosis [Esteva et al., 2017, 2019] or autonomous driving [Caesar et al., 2020, Sun et al., 2020]. In many real world applications it is not only the predictive performance that is important, but also the trustworthiness of the prediction, i.e., we are interested in accurate predictions with robust uncertainty estimates. To this end, it is necessary that the models are uncertainty calibrated, which means that, for instance, among all cells that have been predicted with a probability of 0.8 to be cancerous, 80% should indeed belong to a malignant tumor.

The field of uncertainty calibration has been mostly focused on binary problems, often considering only the confidence score of the predicted class. However, this so called top-label (or confidence) calibration [Guo et al., 2017]) is often not sufficient in multiclass settings. A stronger notion of

*Equal contribution

[†]Most of this work was done while at KU Leuven

Table 1: Properties of ECE^{KDE} and other commonly used calibration error estimators.

	Properties			
	Consistency	Scalability	De-biased	Differentiable
ECE^{KDE} (Our)	✓	✓	✓	✓
ECE^{bin}	✗ [Vaicenavicius et al., 2019]	✗	✓ [Roelofs et al., 2022]	✗
Mix-n-Match	✓ [Zhang et al., 2020]	✗	✗	✓
MMCE	✗ [Kumar et al., 2018]	✓	✗	✓

calibration is marginal (or class-wise) [Kull et al., 2019], that splits up the multiclass problem into K one-vs-all binary ones, and requires each to be calibrated according to the definition of binary calibration. The most strict notion of calibration, called canonical (or distribution) calibration [Bröcker, 2009, Kull and Flach, 2015, Vaicenavicius et al., 2019], requires the whole probability vector to be calibrated. The curse of dimensionality makes estimation of this form of calibration difficult, and current estimators, such as the binned estimator ECE^{bin} [Naeini et al., 2015], MMCE [Kumar et al., 2018] and Mix-n-Match [Zhang et al., 2020], have computational or statistical limitations that prevent them from being successfully applied in this important setting. Specifically, the binned estimator is sensitive to the binning scheme and is asymptotically inconsistent in many situations Vaicenavicius et al. [2019], MMCE is not a consistent estimator of L_p calibration error and Mix-n-Match, although consistent, is intractable in high dimensions and the authors did not implement it in more than one dimension.

We propose a tractable, differentiable, and consistent estimator of the expected L_p canonical calibration error. In particular, we use kernel density estimates (KDEs) with a Beta kernel in binary classification tasks and a Dirichlet kernel in the multiclass setting, as these kernels are the natural choices to model densities over a probability simplex. In Table 1, we summarize and compare the properties of our ECE^{KDE} estimator and other commonly used estimators. ECE^{KDE} scales well to higher dimensions and it is able to capture canonical calibration with $\mathcal{O}(n^2)$ complexity.

Our contributions can be summarized as follows: 1. We develop a tractable estimator of canonical L_p calibration error that is consistent and differentiable. 2. We demonstrate a natural choice of kernel. Due to the scaling properties of Dirichlet kernel density estimation, evaluating *canonical calibration* becomes feasible in cases that cannot be estimated using other methods. 3. We provide a second order debiasing scheme to further improve the convergence of the estimator. 4. We empirically evaluate the correctness of our estimator and demonstrate its utility in the task of calibration regularized risk minimization on variety of network architectures and several datasets.

2 Related Work

Calibration of probabilistic predictors has long been studied in many fields. This topic gained attention in the deep learning community since Guo et al. [2017] observed that modern neural networks are poorly calibrated and tend to give overconfident predictions due to overfitting on the NLL loss. The surge of interest resulted in many calibration strategies that can be split in two general categories, which we discuss subsequently.

Post-hoc calibration strategies learn a calibration map of the predictions from a trained predictor in a post-hoc manner, using a held-out calibration set. For instance, Platt scaling [Platt, 1999] fits a logistic regression model on top of the logit outputs of the model. A special case of Platt scaling that fits a single scalar, called temperature, has been popularized by Guo et al. [2017] as an accuracy-preserving, easy to implement and effective method to improve calibration. However, it has the undesired consequence that it clamps the high confidence scores of accurate predictions [Kumar et al., 2018]. Similar approaches for post-hoc calibration include histogram binning [Zadrozny and Elkan, 2001], isotonic regression [Zadrozny and Elkan, 2002], Bayesian binning into quantiles [Naeini and Cooper, 2016], Beta [Kull et al., 2017] and Dirichlet calibration [Kull et al., 2019]. Recently, Gupta et al. [2021] proposed a binning-free calibration measure based on the Kolmogorov-Smirnov test. In this approach, the recalibration function is obtained via spline-fitting, rather than minimizing a loss function on a calibration set. Ma et al. [2021] integrate ensemble-based and post-hoc calibration methods in an accuracy-perserving truth discovery framework. Zhao et al. [2021] introduce a new

notion of calibration, called decision calibration, however, they do not propose an estimator of calibration error with statistical guarantees.

Trainable calibration strategies integrate a differentiable calibration measure into the training objective. One of the earliest approaches is regularization by penalizing low entropy predictions [Pereyra et al., 2017]. Similarly to temperature scaling, it has been shown that entropy regularization needlessly suppresses high confidence scores of correct predictions [Kumar et al., 2018]. Another popular strategy is MMCE (Maximum Mean Calibration Error) [Kumar et al., 2018], where the entropy regularizer is replaced by a kernel-based surrogate for the calibration error that can be optimized alongside NLL. It has been shown that label smoothing [Szegedy et al., 2016, Müller et al., 2019], i.e. training models with a weighted mixture of the labels instead of one-hot vectors, also improves model calibration. Liang et al. [2020] propose to add the difference between predicted confidence and accuracy as auxiliary term to the cross-entropy loss. Focal loss [Mukhoti et al., 2020, Lin et al., 2017] has recently been *empirically* shown to produce better calibrated models than many of the alternatives, but does not estimate a clear quantity related to calibration error. Bohdal et al. [2021] derive a differentiable approximation to the commonly-used binned estimator of calibration error by computing differentiable approximations to the 0/1 loss and the binning operator. However, this approach does not eliminate the dependence on the binning scheme and it is not clear how it can be extended to calibration of the whole probability vector.

Kernel density estimation [Parzen, 1962, Rosenblatt, 1956, Silverman, 1986] is a non-parametric method to estimate a probability density function from a finite sample. Zhang et al. [2020] propose a KDE-based estimator of the calibration error (Mix-n-Match) for measuring calibration performance. Although they demonstrate consistency of the method, it requires a numerical integration step that is infeasible in high dimensions. In practice, they only implemented binary calibration, and not canonical calibration.

Although many calibration strategies have been empirically shown to decrease the calibration error, very few of them are based on an estimator of miscalibration. Our estimator is the first consistent, differentiable estimator with favourable scaling properties that has been successfully applied to the estimation of L_p canonical calibration error in the multi-class setting.

3 Methods

We study a classical supervised classification problem. Let $(\Omega, \mathcal{A}, \mathbb{P})$ be a probability space, where Ω is the set of possible outcomes, $\mathcal{A} = \mathcal{A}(\Omega)$ is the sigma field of events and $\mathbb{P} : \mathcal{A} \rightarrow [0, 1]$ is a probability measure, let $\mathcal{X} = \mathbb{R}^d$ and $\mathcal{Y} = \{1, \dots, K\}$. Let $x : \Omega \rightarrow \mathcal{X}$ and $y : \Omega \rightarrow \mathcal{Y}$ be random variables, while realizations are denoted with subscripts. Suppose we have a model $f : \mathcal{X} \rightarrow \Delta^K$, where Δ^K denotes the $K - 1$ dimensional simplex as obtained, e.g., from the output of a final softmax layer in a neural network. We measure the (mis-)calibration in terms of the L_p calibration error, defined below.

Definition 3.1 (Calibration error, [Naeini et al., 2015, Kumar et al., 2019, Wenger et al., 2020]). The L_p calibration error of f is:

$$\text{CE}_p(f) = \left(\mathbb{E} \left[\left\| \mathbb{E}[y | f(x)] - f(x) \right\|_p^p \right] \right)^{\frac{1}{p}}. \quad (1)$$

We note that we consider multiclass calibration, and that $f(x)$ and the conditional expectation in Equation (1) therefore map to points on a probability simplex. We say that a classifier f is perfectly calibrated if $\text{CE}_p(f) = 0$.

In order to empirically compute the conditional expectation in Equation (1), we need to perform density estimation over the probability simplex. In a binary setting, this has traditionally been done with binned estimates [Naeini et al., 2015, Guo et al., 2017, Kumar et al., 2019]. However, this is not differentiable w.r.t. the function f , and cannot be incorporated into a gradient based training procedure. Furthermore, binned estimates suffer from the curse of dimensionality and do not have a practical extension to multiclass settings. We consider an estimator for the CE_p based on Beta and Dirichlet kernel density estimates in the binary and multiclass setting, respectively. We require that this estimator is consistent and differentiable such that we can train it in a calibration error regularized

risk minimization framework. This estimator is given by:

$$\widehat{\text{CE}}_p(f)^p = \frac{1}{n} \sum_{j=1}^n \left[\left\| \mathbb{E}[y | \widehat{f}(x)] \Big|_{f(x_j)} - f(x_j) \right\|_p^p \right], \quad (2)$$

where $\mathbb{E}[y | \widehat{f}(x)] \Big|_{f(x_j)}$ denotes $\mathbb{E}[y | \widehat{f}(x)]$ evaluated at $f(x) = f(x_j)$. If probability density $p_{x,y}$ is measurable with respect to the product of the Lebesgue and counting measure, we can define: $p_{x,y}(x_i, y_i) = p_{y|x=x_i}(y_i) p_x(x_i)$. Then we define the estimator of the conditional expectation as follows:

$$\begin{aligned} \mathbb{E}[y | f(x)] &= \sum_{y_k \in \mathcal{Y}} y_k p_{y|f(x)}(y_k) = \frac{\sum_{y_k \in \mathcal{Y}} y_k p_{f(x),y}(f(x), y_k)}{p_{f(x)}(f(x))} \\ &\approx \frac{\sum_{i=1}^n k(f(x); f(x_i)) y_i}{\sum_{i=1}^n k(f(x); f(x_i))} =: \widehat{\mathbb{E}}[y | f(x)] \end{aligned} \quad (3)$$

where k is the kernel of a kernel density estimate evaluated at point x and $p_{f(x)}$ is uniquely determined by p_x and f .

Proposition 3.2. *Assuming that $p_{f(x)}(f(x))$ is Lipschitz continuous over the interior of the simplex, there exists a kernel k such that $\widehat{\mathbb{E}}[y | f(x)]$ is a pointwise consistent estimator of $\mathbb{E}[y | f(x)]$, that is:*

$$\text{plim}_{n \rightarrow \infty} \frac{\sum_{i=1}^n k(f(x); f(x_i)) y_i}{\sum_{i=1}^n k(f(x); f(x_i))} = \frac{\sum_{y_k \in \mathcal{Y}} y_k p_{f(x),y}(f(x), y_k)}{p_{f(x)}(f(x))}. \quad (4)$$

Proof. Let k be a Dirichlet kernel [Ouimet and Tolosana-Delgado, 2022]. By the consistency of the Dirichlet kernel density estimators [Ouimet and Tolosana-Delgado, 2022, Theorem 4] Lipschitz continuity of the density over the simplex is a sufficient condition for uniform convergence of the kernel density estimate. This in turn implies that for a given f , for all $f(x) \in (0, 1)$, $\frac{1}{n} \sum_{i=1}^n k(f(x); f(x_i)) y_i \xrightarrow{P} \sum_{y_k \in \mathcal{Y}} y_k p_{f(x),y}(f(x), y_k)$ and $\frac{1}{n} \sum_{i=1}^n k(f(x); f(x_i)) \xrightarrow{P} p_{f(x)}(f(x))$. Let $g(x) = 1/x$, then the set of discontinuities of g applied to the denominator of the l.h.s. of (4) has measure zero since $\frac{1}{n} \sum_{i=1}^n k(f(x); f(x_i)) = 0$ with probability zero. From the continuous mapping theorem [Mann and Wald, 1943] it follows, that $n/(\sum_{i=1}^n k(f(x); f(x_i))) \xrightarrow{P} 1/p_{f(x)}(f(x))$. Since products of convergent (in probability) sequences of random variables converge in probability to the product of their limits [Resnick, 2019], we have that $\sum_{i=1}^n k(f(x); f(x_i)) y_i g(\sum_{i=1}^n k(f(x); f(x_i))) \xrightarrow{P} \sum_{y_k \in \mathcal{Y}} y_k p_{f(x),y}(f(x), y_k) g(p_{f(x)}(f(x)))$, which is equal to the r.h.s. of (4). \square

The most commonly used loss functions are designed to achieve consistency in the sense of Bayes optimality under risk minimization, however, they do not guarantee calibration - neither for finite samples nor in the asymptotic limit. Since we are interested in models f that are both accurate and calibrated, we consider the following optimization problem bounding the calibration error $\text{CE}(f)$: $f = \arg \min_{f \in \mathcal{F}} \text{Risk}(f)$, s.t. $\text{CE}(f) \leq B$ for some $B > 0$, and its associated Lagrangian

$$f = \arg \min_{f \in \mathcal{F}} \left(\text{Risk}(f) + \lambda \cdot \text{CE}(f) \right). \quad (5)$$

Mean squared error in binary classification As a first instantiation of our framework we consider a binary classification setting, with mean squared error $\text{MSE}(f) = \mathbb{E}[(f(x) - y)^2]$ as the risk function, jointly optimized with the L_2 calibration error CE_2 :

$$f = \arg \min_{f \in \mathcal{F}} \left(\text{MSE}(f) + \lambda \text{CE}_2(f)^2 \right) = \arg \min_{f \in \mathcal{F}} \left(\text{MSE}(f) + \gamma \mathbb{E} \left[\mathbb{E}[y | f(x)]^2 \right] \right) \quad (6)$$

where $\gamma = \frac{\lambda}{\lambda+1} \in [0, 1)$. The full derivation using the MSE decomposition [Murphy, 1973, Degroot and Fienberg, 1983, Kuleshov and Liang, 2015, Nguyen and O'Connor, 2015] is given in Appendix

A. For optimization we wish to find an estimator for $\mathbb{E}[\mathbb{E}[y | f(x)]^2]$. Building upon Equation (3), a partially debiased estimator can be written as:

$$\mathbb{E}\left[\widehat{\mathbb{E}[y | f(x)]^2}\right] \approx \frac{1}{n} \sum_{j=1}^n \frac{\left(\sum_{i \neq j} k(f(x_j); f(x_i)) y_i\right)^2 - \sum_{i \neq j} (k(f(x_j); f(x_i)) y_i)^2}{\left(\sum_{i \neq j} k(f(x_j); f(x_i))\right)^2 - \sum_{i \neq j} (k(f(x_j); f(x_i)))^2}. \quad (7)$$

Thus, the conditional expectation is estimated using a ratio of unbiased estimators of the square of a mean.

Proposition 3.3. Equation (7) is a ratio of two U-statistics and has a bias converging as $\mathcal{O}\left(\frac{1}{n}\right)$.

The proof is given in Appendix B.

Proposition 3.4. There exist de-biasing schemes for the ratios in Equation (7) and Equation (3) that achieve an improved $\mathcal{O}\left(\frac{1}{n^2}\right)$ convergence of the bias.

Proofs are given in Appendix C and D.

In a binary setting, the kernels $k(\cdot, \cdot)$ are Beta distributions defined as:

$$k_B(f(x_j), f(x_i)) := f(x_j)^{\alpha_i - 1} (1 - f(x_j))^{\beta_i - 1} \frac{\Gamma(\alpha_i + \beta_i)}{\Gamma(\alpha_i) \Gamma(\beta_i)}, \quad (8)$$

with $\alpha_i = \frac{f(x_i)}{h} + 1$ and $\beta_i = \frac{1 - f(x_i)}{h} + 1$ [Chen, 1999, Bouezmarni and Rolin, 2003, Zhang and Karunamuni, 2010], where h is a bandwidth parameter in the kernel density estimate that goes to 0 as $n \rightarrow \infty$. We note that the computational complexity of this estimator is $\mathcal{O}(n^2)$. If we would use this within a gradient descent training procedure, the density can be estimated using a mini-batch and therefore the $\mathcal{O}(n^2)$ complexity is w.r.t. the size of a mini-batch, not the entire dataset.

The estimator in Equation (7) is a ratio of two second order U-statistics that converge as $n^{-1/2}$ [Ferguson, 2005]. Therefore, the overall convergence will be $n^{-1/2}$. Empirical convergence rates are calculated in Appendix G and shown to be close to the theoretically expected value.

Multiclass calibration with Dirichlet kernel density estimates There are multiple definitions regarding multiclass calibration that differ in the strictness regarding the calibration of the probability vector $f(x)$. The strongest notion of multiclass calibration, and the one that we consider in this paper, is canonical (also called multiclass or distribution) calibration [Bröcker, 2009, Kull and Flach, 2015, Vaicenavicius et al., 2019], which requires that the whole probability vector $f(x)$ is calibrated (Definition 3.1). Its estimator is:

$$\widehat{\text{CE}}_p(f)^p = \frac{1}{n} \sum_{j=1}^n \left\| \frac{\sum_{i \neq j} k_{\text{Dir}}(f(x_j); f(x_i)) y_i}{\sum_{i \neq j} k_{\text{Dir}}(f(x_j); f(x_i))} - f(x_j) \right\|_p^p \quad (9)$$

where k_{Dir} is a Dirichlet kernel defined as:

$$k_{\text{Dir}}(f(x_j), f(x_i)) = \frac{\Gamma(\sum_{k=1}^K \alpha_{ik})}{\prod_{k=1}^K \Gamma(\alpha_{ik})} \prod_{k=1}^K f(x_j)^{\alpha_{ik} - 1} \quad (10)$$

with $\alpha_i = \frac{f(x_i)}{h} + 1$ [Ouimet and Tolosana-Delgado, 2022]. As before, the computational complexity is $\mathcal{O}(n^2)$ irrespective of p .

This estimator is differentiable and furthermore, the following proposition holds:

Proposition 3.5. The Dirichlet kernel based CE estimator is consistent when $p_{f(x)}(f(x))$ is Lipschitz:

$$\text{plim}_{n \rightarrow \infty} \frac{1}{n} \sum_{j=1}^n \left\| \frac{\sum_{i \neq j} k_{\text{Dir}}(f(x_j); f(x_i)) y_i}{\sum_{i \neq j} k_{\text{Dir}}(f(x_j); f(x_i))} - f(x_j) \right\|_p^p = \mathbb{E} \left[\left\| \mathbb{E}[y | f(x)] - f(x) \right\|_p^p \right]^p.$$

Proof. Dirichlet kernel estimators are consistent when the density is Lipschitz continuous over the simplex [Ouimet and Tolosana-Delgado, 2022, Theorem 4], consequently, by Proposition 3.2 the

term inside the norm is consistent for any fixed $f(x_j)$ (note, that summing over $i \neq j$ ensures that the ratio of the KDE’s does not depend on the outer summation). Moreover, for any convergent sequence also the norm of that sequence converges to the norm of its limit. Ultimately, the outer sum is merely the sample mean of consistent summands, which again is consistent. \square

With this development, we have for the first time a consistent, differentiable, tractable estimator of L_p canonical calibration error with $\mathcal{O}(n^2)$ computational cost and $\mathcal{O}(n^{-1/2})$ convergence rate, with a debiasing scheme that achieves $\mathcal{O}(n^{-2})$ bias for $p \in \{1, 2\}$.

4 Empirical validation of ECE^{KDE}

Accurately evaluating the calibration error is a crucial step towards designing trustworthy models that can be used in societally important settings. The most widely used metric for evaluating miscalibration, and the only other estimator that can be straightforwardly extended to measure canonical calibration, is the histogram-based estimator ECE^{bin} . However, as discussed in Vaicenavicius et al. [2019], Widmann et al. [2019], Ding et al. [2020], Ashukha et al. [2020], it has numerous flaws, such as: (i) it is sensitive to the binning scheme (ii) it is severely affected by the curse of dimensionality, as the number of bins grows exponentially with the number of classes (iii) it is asymptotically inconsistent in many cases.

To investigate its relationship with our estimator ECE^{KDE} , we first introduce an extension of the top-label binned estimator to the probability simplex in the three class setting. We start by partitioning the probability simplex into equally-sized, triangle-shaped bins and assign the probability scores to the corresponding bin, as shown in Figure 1a. Then, we define the binned estimate of canonical calibration error as follows: $CE_p(f)^p \approx \mathbb{E} \left[\|H(f(x)) - f(x)\|_p^p \right] \approx \frac{1}{n} \sum_{i=1}^n \|H(f(x_i)) - f(x_i)\|_p^p$, where $H(f(x_i))$ is the histogram estimate, shown in Figure 1b. The surface of the corresponding Dirichlet KDE is presented in Figure 1c. See Appendix F for (i) an experiment investigating their relationship for the three types of calibration (top-label, marginal, canonical) and with varying number of points used for the estimation, and (ii) another example of the binned estimator and Dirichlet KDE on CIFAR-10.

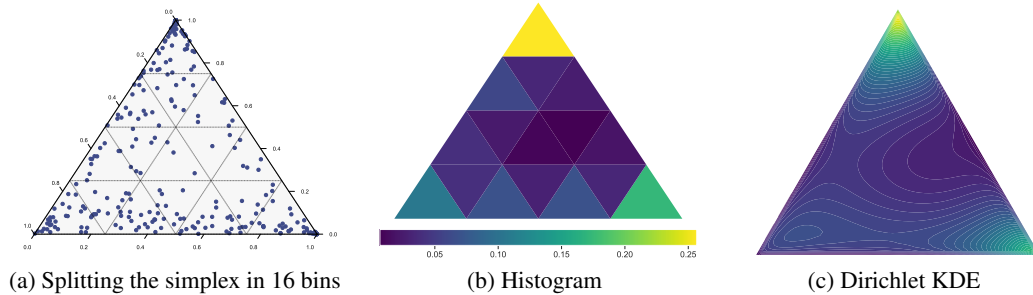


Figure 1: Extension of the binned estimator ECE^{bin} to the probability simplex, compared with the ECE^{KDE} . The ECE^{KDE} achieves a better approximation to the finite sample, and accurately models the fact that samples tend to be concentrated near low dimensional faces of the simplex.

Synthetic experiments We consider an extension of ECE^{bin} to arbitrary number of classes and investigate its performance compared to ECE^{KDE} . Since on real data the ground truth calibration error is unknown, we generate synthetic data with known transformations with the following procedure. First, we sample uniformly from the simplex using the Kraemer algorithm [Smith and Tromble, 2004]. Then, we apply temperature scaling with $t_1 = 0.6$ to simulate realistic scenarios where the probability scores are concentrated along lower dimensional faces of the simplex. We generate ground truth labels according to the sampled probabilities and therefore obtain a perfectly calibrated classifier. Subsequently, the classifier is miscalibrated by additional temperature scaling with $t_2 = 0.6$. Figure 2a depicts the performance of the two estimators as a function of the sample size on generated data for 4 and 8 classes. ECE^{KDE} converges to the ground truth value obtained

by integration in both cases, whereas ECE^{bin} provides poor estimates even with 20000 points. In another experiment with synthetic data we look at the bias of the sharpness³ term in a binary setting. In Figure 2b we plot the estimated value of the sharpness term for varying number of samples, both using the partially debiased ratio from Equation (7) and the ratio debiased with the scheme introduced in Appendix D. A sigmoidal function is applied to the calibrated data to obtain an uncalibrated sample that is used to compute the partially debiased and the fully debiased ratio of the sharpness term. The ground truth value is obtained by using 100 million samples to compute the ratio with the partially debiased version, as it converges asymptotically to the true value due to its consistency. We use a bandwidth of 0.5 and average over 10000 repetitions for each number of samples that range from 32 to 16384. We fix the location of the KDE at $f(x_j) = 0.17$.

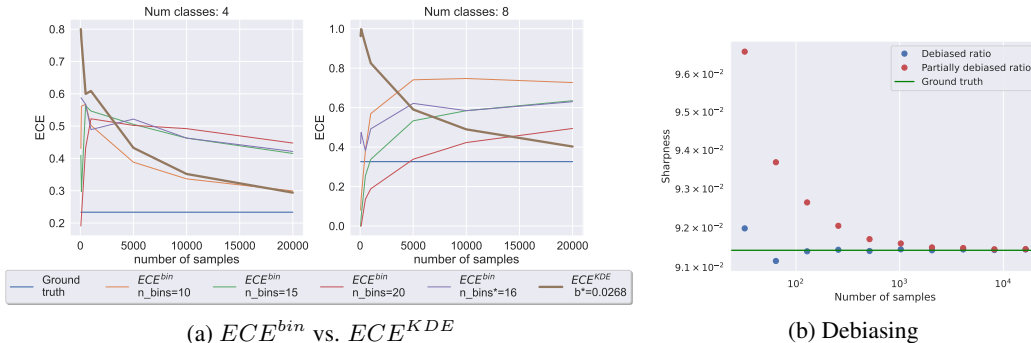


Figure 2: 2a Performance of ECE^{bin} and ECE^{KDE} on synthetic data for varying number of classes, as a function of the sample size. Ground truth represents the true value of the integral. ECE^{bin} is calculated using several common choices for the number of bins (n_bins represents number of bins per-class.) n_bins and b are found as optimal values according to Doane’s formula [Doane, 1976] and LOO MLE, respectively. ECE^{KDE} converges to the true value in all settings, in contrast to ECE^{bin} . 2b Sharpness term evaluated for different numbers of samples with the partially debiased ratio from Equation (7) and with the debiasing scheme derived in Appendix D on synthetic data.

5 Calibration regularized training

Empirical setup To showcase our estimator in applications where canonical calibration is crucial, we consider two medical datasets, namely Kather and DermaMNIST. The Kather dataset [Kather et al., 2016] consists of 5000 histological images of human colorectal cancer and it has eight different classes of tissue. DermaMNIST [Yang et al., 2021] is a pre-processed version of the HAM10000 dataset [Tschandl et al., 2018], containing 10015 dermatoscopic images of skin lesions, categorized in seven classes. Both datasets have been collected in accordance with the Declaration of Helsinki. According to standard practice in related works, we trained ResNet [He et al., 2016], ResNet with stochastic depth (SD) [Huang et al., 2016], DenseNet [Huang et al., 2017] and WideResNet [Zagoruyko and Komodakis, 2016] networks also on CIFAR-10/100 [Krizhevsky, 2009]. We use 45000 images for training on the CIFAR datasets, 4000 for Kather and 7007 for DermaMNIST. The code is available at <https://github.com/tpopordanoska/ece-kde>.

Baselines *Cross-entropy*: The first baseline model is trained using cross-entropy (**XE**), with the data preprocessing, training procedure and hyperparameters described in the corresponding paper for the architecture.

Trainable calibration strategies **KDE-XE** denotes our proposed estimator ECE^{KDE} , as defined in Equation (9), jointly trained with cross entropy. **MMCE** [Kumar et al., 2018] is a differentiable measure of calibration with a property that it is minimized at perfect calibration, i.e., MMCE is 0 if and only if $CE_p = 0$. It is used as a regulariser alongside NLL, with the strength of regularization parameterized by λ . **Focal loss (FL)** [Mukhoti et al., 2020] is an alternative to the cross-entropy loss, defined as $\mathcal{L}_f = -(1 - f(y|x))^\gamma \log(f(y|x))$, where γ is a hyperparameter and $f(y|x)$ is the

³ The sharpness is defined as $\text{Var}(\mathbb{E}[y | f(x)])$ [Kuleshov and Liang, 2015]. Here we neglect the term that does not depend on $f(x)$, and thereby refer to $\mathbb{E}[\mathbb{E}[y | f(x)]^2]$ as the sharpness.

probability score that a neural network f outputs for a class y on an input x . Their best-performing approach is the sample-dependent FL-53 where $\gamma = 5$ for $f(y|x) \in [0, 0.2)$ and $\gamma = 3$ otherwise, followed by the method with fixed $\gamma = 3$.

Post-hoc calibration strategies Guo et al. [2017] investigated the performance of several post-hoc calibration methods and found **temperature scaling** to be a strong baseline, which we use as a representative of this group. It works by scaling the logits with a scalar $T > 0$, typically learned on a validation set by minimizing NLL. Following Kumar et al. [2018], Mukhoti et al. [2020], we also use temperature scaling as a post-processing step for our method.

Metrics We report L_1 canonical calibration using our ECE^{KDE} estimator, calculated according to Equation (9). Additional experiments with L_1 and L_2 top-label calibration on CIFAR-10/100 can be found in Appendix E.

Hyperparameters A crucial parameter for KDE is the bandwidth b , a positive number that defines the smoothness of the density plot. Poorly chosen bandwidth may lead to undersmoothing (small bandwidth) or oversmoothing (large bandwidth), as shown in Figure 3. A commonly used non-parametric bandwidth selector is maximum likelihood cross validation [Duin, 1976]. For our experiments we choose the bandwidth from a list of possible values by maximizing the leave-one-out likelihood (LOO MLE). The λ parameter for weighting the calibration error w.r.t the loss is typically chosen via cross-validation or using a holdout validation set. We found that for KDE-XE, values of $\lambda \in [0.001, 0.2]$ provide a good trade-off in terms of accuracy and calibration error. The p parameter is selected depending on the desired L_p calibration error and the corresponding theoretical guarantees. The rest of the hyperparameters for training are set as proposed in the corresponding papers for the architectures we benchmark. In particular, for the CIFAR-10/100 datasets we used a batch size of 64 for DenseNet and 128 for the other architectures. For the medical datasets, we used a batch size of 64, due to their smaller size.

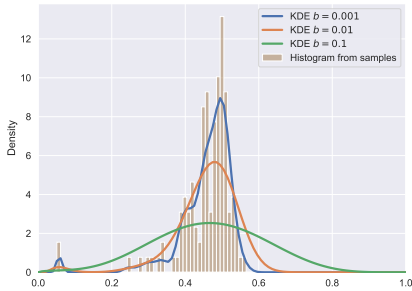


Figure 3: Effect of the bandwidth b on the shape of the estimate.

5.1 Experiments

An important property of our ECE^{KDE} estimator is differentiability, allowing it to be used in a calibration regularized training framework. In this section, we benchmark KDE-XE with several baselines on medical diagnosis applications, where the calibration of the whole probability vector is of particular interest. For completeness, we also include an experiment on CIFAR-10.

Table 2 summarizes the canonical L_1 ECE^{KDE} and Table 3 the accuracy, measured across multiple architectures. The bandwidth is chosen by LOO MLE. For MMCE and KDE-XE the best performing regularization weight is reported. In Table 2 we notice that KDE-XE consistently achieves very competitive ECE values, while also boosting the accuracy, as shown in Table 3. Interestingly, we observe that temperature scaling does not improve canonical calibration error, contrary to its reported improvements on top-label calibration. This observation that temperature scaling is less effective for stronger notions of calibration is consistent with a similar finding in Kull et al. [2019], where the authors show that although the temperature-scaled model has well calibrated top-label confidence scores, the calibration error is much larger for class-wise calibration.

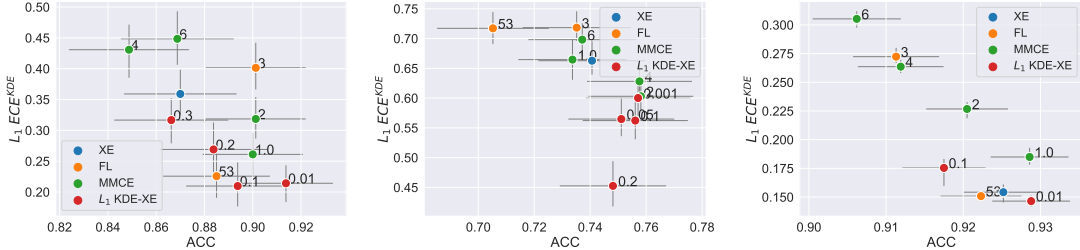
Figure 4 shows the performance of several architectures and datasets in terms of accuracy and L_1 ECE^{KDE} for various choices of the regularization parameter for MMCE and KDE-XE. The 95% confidence intervals for ECE^{KDE} are calculated using 100 and 10 bootstrap samples on the medical datasets and CIFAR-10, respectively. In all settings, KDE-XE Pareto dominates the competitors, for several choices of λ . For example, on DermaMNIST trained with DenseNet, KDE-XE with $\lambda = 0.2$ reduces ECE^{KDE} from 66% to 45%.

Table 2: Canonical L_1 ECE^{KDE} (\downarrow) for different loss functions and architectures, both trained from scratch (Pre T) and after temperature scaling on a validation set (Post T). Best results across Pre T methods are marked in bold.

Dataset	Model	XE		MMCE		FL-53		L_1 KDE-XE (Our)	
		Pre T	Post T	Pre T	Post T	Pre T	Post T	Pre T	Post T
Kather	ResNet-110	0.335	0.304	0.343	0.300	0.325	0.248	0.311	0.289
	ResNet-110 (SD)	0.329	0.334	0.235	0.159	0.209	0.122	0.198	0.147
	Wide-ResNet-28-10	0.177	0.259	0.201	0.241	0.270	0.328	0.162	0.212
	DenseNet-40	0.244	0.251	0.159	0.218	0.165	0.207	0.114	0.154
DermaMNIST	ResNet-110	0.579	0.602	0.575	0.603	0.684	0.618	0.467	0.516
	ResNet-110 (SD)	0.534	0.571	0.470	0.526	0.567	0.594	0.461	0.538
	Wide-ResNet-28-10	0.546	0.599	0.470	0.512	0.623	0.608	0.455	0.599
	DenseNet-40	0.573	0.578	0.514	0.558	0.577	0.557	0.366	0.418
CIFAR-10	ResNet-110	0.133	0.170	0.171	0.196	0.138	0.171	0.126	0.163
	ResNet-110 (SD)	0.132	0.172	0.164	0.203	0.156	0.201	0.178	0.223
	Wide-ResNet-28-10	0.083	0.098	0.143	0.155	0.147	0.177	0.077	0.091
	DenseNet-40	0.104	0.131	0.133	0.155	0.081	0.081	0.090	0.124

Table 3: Accuracy (\uparrow) computed for different architectures. Best results are marked in bold.

Dataset	Model	XE	MMCE	FL-53	L_1 KDE-XE
Kather	ResNet-110	0.840	0.860	0.844	0.860
	ResNet-110 (SD)	0.870	0.900	0.885	0.914
	Wide-ResNet-28-10	0.933	0.899	0.873	0.921
	DenseNet-40	0.913	0.93	0.916	0.941
DermaMNIST	ResNet-110	0.720	0.721	0.674	0.744
	ResNet-110 (SD)	0.743	0.753	0.689	0.764
	Wide-ResNet-28-10	0.736	0.741	0.715	0.754
	DenseNet-40	0.741	0.758	0.705	0.748
CIFAR-10	ResNet-110	0.925	0.929	0.922	0.929
	ResNet-110 (SD)	0.926	0.925	0.92	0.907
	Wide-ResNet-28-10	0.954	0.947	0.936	0.954
	DenseNet-40	0.947	0.944	0.948	0.947



(a) ResNet-110 (SD) on Kather

(b) DenseNet on DermaMNIST

(c) ResNet-110 on CIFAR-10

Figure 4: Canonical calibration on various datasets and architectures. The numbers next to the points denote the value of the regularization parameter. KDE-XE outperforms the competitors, both in terms of accuracy and calibration error, for several choices of λ .

Training time measurements In Table 4 we summarize the running time per epoch of the four architectures, with regularization (KDE-XE) and without regularization (XE). We observe only an insignificant impact on the training speed when using KDE-XE, dispelling any concerns w.r.t. the computational overhead.

To summarize, the experiments show that our estimator is consistently producing competitive calibration errors with other state-of-the-art approaches, while maintaining accuracy and keeping

Table 4: Training time [sec] per epoch for XE and KDE-XE for different models on CIFAR-10.

Dataset	Model	XE	L_1 KDE-XE
CIFAR-10	ResNet-110	51.8	53
	ResNet-110 (SD)	45	46
	Wide-ResNet-28-10	152.9	154.9
	DenseNet-40	103.2	106.8

the computational complexity at $\mathcal{O}(n^2)$. We note that within the proposed calibration-regularized training framework, this complexity is w.r.t. to a mini-batch, and the added cost is less than a couple percent. Furthermore, the $\mathcal{O}(n^2)$ complexity shows up in other related works [Kumar et al., 2018, Zhang et al., 2020], and is intrinsic to the problem of density estimators of calibration error. As a future work, a larger scale benchmarking will be beneficial for exploring the limits of canonical calibration using Dirichlet kernels.

6 Conclusion

In this paper, we proposed a consistent and differentiable estimator of canonical L_p calibration error using Dirichlet kernels. It has favorable computational and statistical properties, with a complexity of $\mathcal{O}(n^2)$, convergence of $\mathcal{O}(n^{-1/2})$ and a bias that converges as $\mathcal{O}(n^{-1})$, which can be further reduced to $\mathcal{O}(n^{-2})$ using our debiasing strategy. The ECE^{KDE} can be directly optimized alongside any loss function in the existing batch stochastic gradient descent framework. Furthermore, we propose using it as a measure of the highest form of calibration, which requires the entire probability vector to be calibrated. To the best of our knowledge, this is the only metric that can tractably capture this type of calibration, which is crucial in safety-critical applications where downstream decisions are made based on the predicted probabilities. We showed empirically on a range of neural architectures and datasets that the performance of our estimator in terms of accuracy and calibration error is competitive against the current state-of-the-art, while having superior properties as a consistent estimator of canonical calibration error.

Acknowledgments

This research received funding from the Research Foundation - Flanders (FWO) through project number S001421N, and the Flemish Government under the ‘‘Onderzoeksprogramma Artificiële Intelligentie (AI) Vlaanderen’’ programme. R.S. was supported in part by the Tübingen AI centre.

Ethical statement

The paper is concerned with estimation of calibration error, a topic for which existing methods are deployed, albeit not typically for canonical calibration error in a multi-class setting. We therefore consider the ethical risks to be effectively the same as for any probabilistic classifier. Experiments apply the method to medical image classification, for which misinterpretation of benchmark results with respect to their clinical applicability has been highlighted as a risk, see e.g. Varoquaux and Cheplygina [2022].

References

- Arsenii Ashukha, Alexander Lyzhov, Dmitry Molchanov, and Dmitry Vetrov. Pitfalls of in-domain uncertainty estimation and ensembling in deep learning. In *International Conference on Learning Representations*, 2020.
- Ondrej Bohdal, Yongxin Yang, and Timothy Hospedales. Meta-calibration: Meta-learning of model calibration using differentiable expected calibration error. *arXiv preprint arXiv:2106.09613*, 2021.
- Taoufik Bouezmarni and Jean-Marie Rolin. Consistency of the beta kernel density function estimator. *The Canadian Journal of Statistics / La Revue Canadienne de Statistique*, 31(1):89–98, 2003.
- Jochen Bröcker. Reliability, sufficiency, and the decomposition of proper scores. *Quarterly Journal of the Royal Meteorological Society*, 135(643):1512–1519, Jul 2009.
- Holger Caesar, Varun Kumar Reddy Bankiti, Alex Lang, Sourabh Vora, Venice Erin Liong, Qiang Xu, Anush Krishnan, Yu Pan, Giancarlo Baldan, and Oscar Beijbom. nuscenes: A multimodal dataset for autonomous driving. In *Proceedings of the IEEE/CVF Conference on Computer Vision and Pattern Recognition*, page 11621–11631, 06 2020.
- Song Xi Chen. Beta kernel estimators for density functions. *Computational Statistics & Data Analysis*, 31:131–145, 1999.

- M. Degroot and S. Fienberg. The comparison and evaluation of forecasters. *The Statistician*, 32: 12–22, 1983.
- Yukun Ding, Jinglan Liu, Jinjun Xiong, and Yiyu Shi. Revisiting the evaluation of uncertainty estimation and its application to explore model complexity-uncertainty trade-off. In *2020 IEEE/CVF Conference on Computer Vision and Pattern Recognition Workshops (CVPRW)*, pages 22–31, 2020.
- David P. Doane. Aesthetic frequency classifications. *The American Statistician*, 30(4):181–183, 1976.
- Robert Duin. On the choice of smoothing parameters for parzen estimators of probability density functions. *IEEE Transactions on Computers*, C-25(11):1175–1179, 1976.
- Andre Esteva, Brett Kopley, Roberto A. Novoa, Justin Ko, Susan M. Swetter, Helen M. Blau, and Sebastian Thrun. Dermatologist-level classification of skin cancer with deep neural networks. *Nature*, 542:115–, 2017.
- Andre Esteva, Alexandre Robicquet, Bharath Ramsundar, Volodymyr Kuleshov, Mark DePristo, Katherine Chou, Claire Cui, Greg Corrado, Sebastian Thrun, and Jeff Dean. A guide to deep learning in healthcare. *Nature Medicine*, 25, 01 2019.
- Thomas S. Ferguson. U-statistics. In *Notes for Statistics 200C*. UCLA, 2005.
- Chuan Guo, Geoff Pleiss, Yu Sun, and Kilian Q Weinberger. On calibration of modern neural networks. In *International conference on machine learning*, pages 1321–1330. PMLR, 2017.
- Kartik Gupta, Amir Rahimi, Thalaiyasingam Ajanthan, Thomas Mensink, Cristian Sminchisescu, and Richard Hartley. Calibration of neural networks using splines. In *International Conference on Learning Representations*, 2021.
- Kaiming He, Xiangyu Zhang, Shaoqing Ren, and Jian Sun. Deep residual learning for image recognition. In *Proceedings of the IEEE conference on computer vision and pattern recognition*, pages 770–778, 2016.
- Gao Huang, Yu Sun, Zhuang Liu, Daniel Sedra, and Kilian Q Weinberger. Deep networks with stochastic depth. In *European conference on computer vision*, pages 646–661. Springer, 2016.
- Gao Huang, Zhuang Liu, Laurens van der Maaten, and Kilian Q. Weinberger. Densely connected convolutional networks. In *Proceedings of the IEEE Conference on Computer Vision and Pattern Recognition (CVPR)*, 2017.
- Jakob Kather, Cleo-Aron Weis, Francesco Bianconi, Susanne Melchers, Lothar Schad, Timo Gaiser, Alexander Marx, and Frank Zöllner. Multi-class texture analysis in colorectal cancer histology. *Scientific Reports*, 6:27988, 06 2016.
- Alex Krizhevsky. Learning multiple layers of features from tiny images. Technical report, University of Toronto, 2009.
- Volodymyr Kuleshov and Percy S Liang. Calibrated structured prediction. In C. Cortes, N. Lawrence, D. Lee, M. Sugiyama, and R. Garnett, editors, *Advances in Neural Information Processing Systems*, volume 28. Curran Associates, Inc., 2015.
- Meelis Kull and Peter Flach. Novel decompositions of proper scoring rules for classification: Score adjustment as precursor to calibration. In *Joint European Conference on Machine Learning and Knowledge Discovery in Databases*, pages 68–85. Springer, 2015.
- Meelis Kull, Telmo Silva Filho, and Peter Flach. Beta calibration: a well-founded and easily implemented improvement on logistic calibration for binary classifiers. In Aarti Singh and Jerry Zhu, editors, *Proceedings of the 20th International Conference on Artificial Intelligence and Statistics*, volume 54 of *Proceedings of Machine Learning Research*, pages 623–631. PMLR, 20–22 Apr 2017.

- Meelis Kull, Miquel Perello Nieto, Markus Kängsepp, Telmo Silva Filho, Hao Song, and Peter Flach. Beyond temperature scaling: Obtaining well-calibrated multi-class probabilities with dirichlet calibration. *Advances in neural information processing systems*, 32, 2019.
- Ananya Kumar, Percy S Liang, and Tengyu Ma. Verified uncertainty calibration. In H. Wallach, H. Larochelle, A. Beygelzimer, F. d'Alché-Buc, E. Fox, and R. Garnett, editors, *Advances in Neural Information Processing Systems 32*, pages 3792–3803. 2019.
- Aviral Kumar, Sunita Sarawagi, and Ujjwal Jain. Trainable calibration measures for neural networks from kernel mean embeddings. In *ICML*, 2018.
- Gongbo Liang, Yu Zhang, Xiaoqin Wang, and Nathan Jacobs. Improved trainable calibration method for neural networks on medical imaging classification. In *British Machine Vision Conference*, 2020.
- Tsung-Yi Lin, Priya Goyal, Ross Girshick, Kaiming He, and Piotr Dollár. Focal loss for dense object detection. In *Proceedings of the IEEE international conference on computer vision*, pages 2980–2988, 2017.
- Chunwei Ma, Ziyun Huang, Jiayi Xian, Mingchen Gao, and Jinhui Xu. Improving uncertainty calibration of deep neural networks via truth discovery and geometric optimization. In Cassio de Campos and Marloes H. Maathuis, editors, *Proceedings of the Thirty-Seventh Conference on Uncertainty in Artificial Intelligence*, volume 161 of *Proceedings of Machine Learning Research*, pages 75–85. PMLR, 27–30 Jul 2021.
- Henry B Mann and Abraham Wald. On stochastic limit and order relationships. *The Annals of Mathematical Statistics*, 14(3):217–226, 1943.
- Jishnu Mukhoti, Viveka Kulharia, Amartya Sanyal, Stuart Golodetz, Philip Torr, and Puneet Dokania. Calibrating deep neural networks using focal loss. *Advances in Neural Information Processing Systems*, 33:15288–15299, 2020.
- Rafael Müller, Simon Kornblith, and Geoffrey E Hinton. When does label smoothing help? *Advances in neural information processing systems*, 32, 2019.
- A. Murphy. A new vector partition of the probability score. *Journal of Applied Meteorology*, 12: 595–600, 1973.
- Mahdi Pakdaman Naeini and Gregory F Cooper. Binary classifier calibration using an ensemble of near isotonic regression models. In *2016 IEEE 16th International Conference on Data Mining (ICDM)*, pages 360–369. IEEE, 2016.
- Mahdi Pakdaman Naeini, Gregory F. Cooper, and Milos Hauskrecht. Obtaining well calibrated probabilities using Bayesian binning. In *Proceedings of the Twenty-Ninth AAAI Conference on Artificial Intelligence*, pages 2901–2907, 2015.
- Khanh Nguyen and Brendan O’Connor. Posterior calibration and exploratory analysis for natural language processing models. *arXiv preprint arXiv:1508.05154*, 2015.
- R.C. Ogliore, G.R. Huss, and K. Nagashima. Ratio estimation in SIMS analysis. *Nuclear Instruments and Methods in Physics Research Section B-beam Interactions With Materials and Atoms*, 269, 06 2011.
- Frédéric Ouimet and Raimon Tolosana-Delgado. Asymptotic properties of dirichlet kernel density estimators. *Journal of Multivariate Analysis*, 187:104832, 2022.
- Emanuel Parzen. On estimation of a probability density function and mode. *The Annals of Mathematical Statistics*, 33(3):1065–1076, 1962.
- Gabriel Pereyra, George Tucker, Jan Chorowski, Łukasz Kaiser, and Geoffrey Hinton. Regularizing neural networks by penalizing confident output distributions. *arXiv preprint arXiv:1701.06548*, 2017.
- John C. Platt. Probabilistic outputs for support vector machines and comparisons to regularized likelihood methods. In *Advances in Large Margin Classifiers*, pages 61–74. MIT Press, 1999.

- Sidney Resnick. *A probability path*. Springer, 2019.
- Rebecca Roelofs, Nicholas Cain, Jonathon Shlens, and Michael C. Mozer. Mitigating bias in calibration error estimation. In Gustau Camps-Valls, Francisco J. R. Ruiz, and Isabel Valera, editors, *Proceedings of The 25th International Conference on Artificial Intelligence and Statistics*, volume 151 of *Proceedings of Machine Learning Research*, pages 4036–4054. PMLR, 28–30 Mar 2022.
- Murray Rosenblatt. Remarks on some nonparametric estimates of a density function. *The Annals of Mathematical Statistics*, 27(3):832 – 837, 1956.
- Jun Shao. *Mathematical Statistics*, page 180. Springer Texts in Statistics, second edition, 2003.
- B. W. Silverman. *Density Estimation for Statistics and Data Analysis*. Chapman & Hall, 1986.
- Noah A. Smith and Roy W. Tromble. *Sampling Uniformly from the Unit Simplex*. 2004.
- Pei Sun, Henrik Kretzschmar, Xerxes Dotiwalla, Aurelien Chouard, Vijaysai Patnaik, Paul Tsui, James Guo, Yin Zhou, Yuning Chai, Benjamin Caine, Vijay Vasudevan, Wei Han, Jiquan Ngiam, Hang Zhao, Aleksei Timofeev, Scott M. Ettinger, Maxim Krivokon, Amy Gao, Aditya Joshi, Yu Zhang, Jonathon Shlens, Zhifeng Chen, and Dragomir Anguelov. Scalability in perception for autonomous driving: Waymo open dataset. *2020 IEEE/CVF Conference on Computer Vision and Pattern Recognition (CVPR)*, pages 2443–2451, 2020.
- Christian Szegedy, Vincent Vanhoucke, Sergey Ioffe, Jon Shlens, and Zbigniew Wojna. Rethinking the inception architecture for computer vision. In *Proceedings of the IEEE conference on computer vision and pattern recognition*, pages 2818–2826, 2016.
- Myint Tin. Comparison of some ratio estimators. *Journal of the American Statistical Association*, 60 (309):294–307, 1965.
- Philipp Tschandl, Cliff Rosendahl, and Harald Kittler. The HAM10000 dataset, a large collection of multi-source dermatoscopic images of common pigmented skin lesions. *Sci. Data*, 5:180161, 2018.
- Juozas Vaicenavicius, David Widmann, Carl Andersson, Fredrik Lindsten, Jacob Roll, and Thomas Schön. Evaluating model calibration in classification. In *The 22nd International Conference on Artificial Intelligence and Statistics*, pages 3459–3467. PMLR, 2019.
- Gaël Varoquaux and Veronika Cheplygina. Machine learning for medical imaging: methodological failures and recommendations for the future. *npj Digital Medicine*, 5:48, 04 2022.
- Jonathan Wenger, Hedvig Kjellström, and Rudolph Triebel. Non-parametric calibration for classification. In *International Conference on Artificial Intelligence and Statistics*, pages 178–190, 2020.
- David Widmann, Fredrik Lindsten, and Dave Zachariah. Calibration tests in multi-class classification: A unifying framework. *Advances in Neural Information Processing Systems*, 32, 2019.
- Jiancheng Yang, Rui Shi, and Bingbing Ni. Medmnist classification decathlon: A lightweight automl benchmark for medical image analysis. *2021 IEEE 18th International Symposium on Biomedical Imaging (ISBI)*, Apr 2021.
- B. Zadrozny and C. Elkan. Transforming classifier scores into accurate multiclass probability estimates. *Proceedings of the eighth ACM SIGKDD international conference on Knowledge discovery and data mining*, 2002.
- Bianca Zadrozny and Charles Elkan. Obtaining calibrated probability estimates from decision trees and naive bayesian classifiers. *ICML*, 1, 05 2001.
- Sergey Zagoruyko and Nikos Komodakis. Wide residual networks. In *British Machine Vision Conference*, 2016.

Jize Zhang, Bhavya Kailkhura, and T. Yong-Jin Han. Mix-n-match: Ensemble and compositional methods for uncertainty calibration in deep learning. In *International Conference on Machine Learning*, 2020.

Shunpu Zhang and Rohana Karunamuni. Boundary performance of the beta kernel estimators. *Journal of Nonparametric Statistics*, 22:81–104, 01 2010.

Shengjia Zhao, Michael Kim, Roshni Sahoo, Tengyu Ma, and Stefano Ermon. Calibrating predictions to decisions: A novel approach to multi-class calibration. In M. Ranzato, A. Beygelzimer, Y. Dauphin, P.S. Liang, and J. Wortman Vaughan, editors, *Advances in Neural Information Processing Systems*, volume 34, pages 22313–22324. Curran Associates, Inc., 2021.

Checklist

1. For all authors...
 - (a) Do the main claims made in the abstract and introduction accurately reflect the paper’s contributions and scope? [\[Yes\]](#)
 - (b) Did you describe the limitations of your work? [\[Yes\]](#)
 - (c) Did you discuss any potential negative societal impacts of your work? [\[Yes\]](#) Please refer to our ethical statement.
 - (d) Have you read the ethics review guidelines and ensured that your paper conforms to them? [\[Yes\]](#)
2. If you are including theoretical results...
 - (a) Did you state the full set of assumptions of all theoretical results? [\[Yes\]](#)
 - (b) Did you include complete proofs of all theoretical results? [\[Yes\]](#)
3. If you ran experiments...
 - (a) Did you include the code, data, and instructions needed to reproduce the main experimental results (either in the supplemental material or as a URL)? [\[Yes\]](#) It is in the supplementary material
 - (b) Did you specify all the training details (e.g., data splits, hyperparameters, how they were chosen)? [\[Yes\]](#)
 - (c) Did you report error bars (e.g., with respect to the random seed after running experiments multiple times)? [\[Yes\]](#) See Figure 4
 - (d) Did you include the total amount of compute and the type of resources used (e.g., type of GPUs, internal cluster, or cloud provider)? [\[Yes\]](#) [\[No\]](#) Table 4 includes compute times. Most of our results are provided in big O complexity.
4. If you are using existing assets (e.g., code, data, models) or curating/releasing new assets...
 - (a) If your work uses existing assets, did you cite the creators? [\[Yes\]](#)
 - (b) Did you mention the license of the assets? [\[No\]](#) We do not release the data. Data license is available via the citation.
 - (c) Did you include any new assets either in the supplemental material or as a URL? [\[No\]](#)
 - (d) Did you discuss whether and how consent was obtained from people whose data you’re using/curating? [\[Yes\]](#) Medical datasets used in this paper conform to the Declaration of Helsinki.
 - (e) Did you discuss whether the data you are using/curating contains personally identifiable information or offensive content? [\[Yes\]](#) Medical datasets used in this paper conform to the Declaration of Helsinki.
5. If you used crowdsourcing or conducted research with human subjects...
 - (a) Did you include the full text of instructions given to participants and screenshots, if applicable? [\[N/A\]](#) We did not use crowdsourcing or conducted research with human subjects
 - (b) Did you describe any potential participant risks, with links to Institutional Review Board (IRB) approvals, if applicable? [\[N/A\]](#) We did not use crowdsourcing or conducted research with human subjects

- (c) Did you include the estimated hourly wage paid to participants and the total amount spent on participant compensation? [N/A] We did not use crowdsourcing or conducted research with human subjects

A Additional derivations

A.1 Derivation of the MSE decomposition

Definition A.1 (Mean Squared Error (MSE)). The mean squared error of an estimator is

$$\text{MSE}(f) := \mathbb{E}[(f(x) - y)^2]. \quad (11)$$

Proposition A.2. $\text{MSE}(f) \geq \text{CE}_2(f)^2$

Proof.

$$\text{MSE}(f) := \mathbb{E}[(f(x) - y)^2] = \mathbb{E}[(f(x) - \mathbb{E}[y | f(x)]) + (\mathbb{E}[y | f(x)] - y)^2] \quad (12)$$

$$= \underbrace{\mathbb{E}[(f(x) - \mathbb{E}[y | f(x)])^2]}_{=\text{CE}_2^2} + \mathbb{E}[(\mathbb{E}[y | f(x)] - y)^2] \quad (13)$$

$$+ 2\mathbb{E}[(f(x) - \mathbb{E}[y | f(x)])(\mathbb{E}[y | f(x)] - y)]$$

which implies

$$\text{MSE}(f) - \text{CE}_2(f)^2 = \mathbb{E}[(\mathbb{E}[y | f(x)] - y)^2] \quad (14)$$

$$+ 2\mathbb{E}[(f(x) - \mathbb{E}[y | f(x)])(\mathbb{E}[y | f(x)] - y)] \quad (15)$$

$$= \mathbb{E}[(\mathbb{E}[y | f(x)] - y)^2] + 2\mathbb{E}[(f(x)\mathbb{E}[y | f(x)] - 2\mathbb{E}[f(x)y] - 2\mathbb{E}[\mathbb{E}[y | f(x)]^2] + 2\mathbb{E}[\mathbb{E}[y | f(x)]y])]$$

$$= \mathbb{E}[\mathbb{E}[y | f(x)]^2] + \mathbb{E}[y^2] - 2\mathbb{E}[\mathbb{E}[y | f(x)]y] \quad (16)$$

$$+ 2\mathbb{E}[(f(x)\mathbb{E}[y | f(x)] - 2\mathbb{E}[f(x)y] - 2\mathbb{E}[\mathbb{E}[y | f(x)]^2] + 2\mathbb{E}[\mathbb{E}[y | f(x)]y])]$$

$$= \mathbb{E}[y^2] + 2\mathbb{E}[(f(x)\mathbb{E}[y | f(x)] - 2\mathbb{E}[f(x)y] - \mathbb{E}[\mathbb{E}[y | f(x)]^2])]$$

$$= \mathbb{E}[(2f(x) - y - \mathbb{E}[y | f(x)])(\mathbb{E}[y | f(x)] - y)] \quad (18)$$

$$= \mathbb{E}[(f(x) - y)(\mathbb{E}[y | f(x)] - y)] \quad (19)$$

$$+ \mathbb{E}[(f(x) - \mathbb{E}[y | f(x)])(\mathbb{E}[y | f(x)] - y)].$$

By the law of total expectation, we will write the above as

$$\text{MSE}(f) - \text{CE}_2(f)^2 = \mathbb{E}[\mathbb{E}[(f(x) - y)(\mathbb{E}[y | f(x)] - y) + (f(x) - \mathbb{E}[y | f(x)])(\mathbb{E}[y | f(x)] - y) | f(x)]]]. \quad (20)$$

Focusing on the inner conditional expectation, we have that

$$\begin{aligned} & \mathbb{E}[(f(x) - y)(\mathbb{E}[y | f(x)] - y) + (f(x) - \mathbb{E}[y | f(x)])(\mathbb{E}[y | f(x)] - y) | f(x)] \\ &= \mathbb{E}[y | f(x)](f(x) - 1)(\mathbb{E}[y | f(x)] - 1) + (1 - \mathbb{E}[y | f(x)])f(x)\mathbb{E}[y | f(x)] \\ & \quad + \mathbb{E}[y | f(x)](f(x) - \mathbb{E}[y | f(x)])(\mathbb{E}[y | f(x)] - 1) \\ & \quad + (1 - \mathbb{E}[y | f(x)])(f(x) - \mathbb{E}[y | f(x)])\mathbb{E}[y | f(x)] \end{aligned} \quad (21)$$

$$= (1 - \mathbb{E}[y | f(x)])\mathbb{E}[y | f(x)] \geq 0 \quad \forall f(x) \quad (22)$$

and therefore

$$\text{MSE}(f) - \text{CE}_2(f)^2 = \mathbb{E}[(1 - \mathbb{E}[y | f(x)])\mathbb{E}[y | f(x)]] \geq 0. \quad (23)$$

□

The expectation in Equation (23) is over variances of Bernoulli random variables with probabilities $\mathbb{E}[y | f(x)]$.

A.2 Derivation of Equation (3)

By considering $y \in \{0, 1\}$, we have the following:

$$\mathbb{E}[y | f(x)] = \sum_{y_k \in \mathcal{Y}} y_k p_{y|f(x)}(y_k) = \frac{\sum_{y_k \in \mathcal{Y}} y_k p_{f(x),y}(f(x), y_k)}{p_{f(x)}(f(x))} \quad (24)$$

$$= \frac{p_{f(x),y}(f(x), y_k = 1)}{p_{f(x)}(f(x))} = \frac{p_{f(x)|y}(f(x)|y_k = 1)p_y(y_k = 1)}{p_{f(x)}(f(x))} \quad (25)$$

$$\approx \frac{\frac{1}{\sum_{i=1}^n y_i} \sum_{i=1}^n k(f(x); f(x_i)) y_i \frac{\sum_{i=1}^n y_i}{n}}{\frac{1}{n} \sum_{i=1}^n k(f(x); f(x_i))} \quad (26)$$

$$\approx \frac{\sum_{i=1}^n k(f(x); f(x_i)) y_i}{\sum_{i=1}^n k(f(x); f(x_i))} =: \mathbb{E}[\widehat{y} | f(x)] \quad (27)$$

A.3 Derivation of Equation (6)

We consider the optimization problem for some $\lambda > 0$:

$$f = \arg \min_{f \in \mathcal{F}} \left(\text{MSE}(f) + \lambda \text{CE}_2(f)^2 \right). \quad (28)$$

Using Equation (23) we rewrite:

$$\begin{aligned} \text{MSE}(f) + \lambda \text{CE}_2(f)^2 &= (1 + \lambda) \text{MSE}(f) - \lambda \left(\text{MSE}(f) - \text{CE}_2(f)^2 \right) \\ &= (1 + \lambda) \text{MSE}(f) - \lambda \mathbb{E} \left[\left(1 - \mathbb{E}[y | f(x)] \right) \mathbb{E}[y | f(x)] \right]. \end{aligned} \quad (29)$$

Rescaling Equation (29) by a factor of $(1 + \lambda)^{-1}$ and a variable substitution $\gamma = \frac{\lambda}{1 + \lambda} \in [0, 1)$, we have that:

$$\begin{aligned} f &= \arg \min_{f \in \mathcal{F}} \left(\text{MSE}(f) + \lambda \text{CE}_2(f)^2 \right) \\ &= \arg \min_{f \in \mathcal{F}} \left(\text{MSE}(f) - \gamma \mathbb{E} \left[\left(1 - \mathbb{E}[y | f(x)] \right) \mathbb{E}[y | f(x)] \right] \right) \\ &= \arg \min_{f \in \mathcal{F}} \left(\text{MSE}(f) + \gamma \mathbb{E} \left[\mathbb{E}[y | f(x)]^2 \right] \right). \end{aligned} \quad (30)$$

B Bias of ratio of U-statistics

The unbiased estimator for the square of a mean μ_X^2 is given by:

$$\widehat{\mu_X^2} = \frac{1}{n(n-1)} \sum_{i=1}^n \sum_{\substack{j=1 \\ j \neq i}}^n X_i X_j = \frac{1}{n(n-1)} \left(\left(\sum_{i=1}^n X_i \right)^2 - \sum_{i=1}^n X_i^2 \right). \quad (31)$$

This is a second order U-statistics with kernel $h(x_1, x_2) = x_1 x_2$. The bias of the ratio of two of these estimators converges as $\mathcal{O}\left(\frac{1}{n}\right)$, as the following lemma proves.

Lemma B.1. *Let θ_1 and θ_2 be two estimable parameters and let U_1 and U_2 be the two corresponding U-statistics of order m_1 and m_2 , respectively, based on a sample of n i.i.d. RVs. The bias of the ratio U_1/U_2 of these two U-statistics will converge as $\mathcal{O}\left(\frac{1}{n}\right)$.*

Proof. Let $R = \theta_1/\theta_2$ be the ratio of two estimable parameters and $r = U_1/U_2$ the ratio of the corresponding U-statistics. Note, that U_i is an unbiased estimator of θ_i , $\mathbb{E}[U_i] = \theta_i$, $i = 1, 2$, however, the ratio is usually biased. To investigate the bias of that ratio we rewrite

$$r = R \left(1 + \frac{U_1 - \theta_1}{\theta_1} \right) \left(1 + \frac{U_2 - \theta_2}{\theta_2} \right)^{-1}. \quad (32)$$

If $\left| \frac{U_2 - \theta_2}{\theta_2} \right| < 1$, we can expand $\left(1 + \frac{U_2 - \theta_2}{\theta_2} \right)^{-1}$ in a geometric series:

$$r = R \left(1 + \frac{(U_1 - \theta_1)}{\theta_1} \right) \left(1 - \frac{(U_2 - \theta_2)}{\theta_2} + \frac{(U_2 - \theta_2)^2}{\theta_2^2} - \frac{(U_2 - \theta_2)^3}{\theta_2^3} + \frac{(U_2 - \theta_2)^4}{\theta_2^4} - \dots \right) \quad (33)$$

$$\begin{aligned} &= R \left(1 + \frac{(U_1 - \theta_1)}{\theta_1} - \frac{(U_2 - \theta_2)}{\theta_2} - \frac{(U_2 - \theta_2)(U_1 - \theta_1)}{\theta_2 \theta_1} \right. \\ &\quad + \frac{(U_2 - \theta_2)^2}{\theta_2^2} + \frac{(U_2 - \theta_2)^2 (U_1 - \theta_1)}{\theta_2^2 \theta_1} - \frac{(U_2 - \theta_2)^3}{\theta_2^3} - \frac{(U_2 - \theta_2)^3 (U_1 - \theta_1)}{\theta_2^3 \theta_1} \\ &\quad \left. + \frac{(U_2 - \theta_2)^4}{\theta_2^4} + \frac{(U_2 - \theta_2)^4 (U_1 - \theta_1)}{\theta_2^4 \theta_1} - \dots \right). \end{aligned} \quad (34)$$

If $\zeta_1 > 0$, a U-statistic U of order m obtained from a sample of n observations converges in distribution [Shao, 2003]:

$$\sqrt{n} (U - \mathbb{E}[U]) \xrightarrow{d} N(0, m^2 \zeta_1). \quad (35)$$

Keeping the terms up to $\Theta\left(\frac{1}{n}\right)$:

$$r = R \left(1 + \frac{(U_1 - \theta_1)}{\theta_1} - \frac{(U_2 - \theta_2)}{\theta_2} - \frac{(U_2 - \theta_2)(U_1 - \theta_1)}{\theta_2 \theta_1} + \frac{(U_2 - \theta_2)^2}{\theta_2^2} + o\left(\frac{1}{n}\right) \right) \quad (36)$$

To examine the bias, we take the expectation value of this expression:

$$\mathbb{E}[r] = R \left(1 + \frac{\mathbb{E}[(U_1 - \theta_1)]}{\theta_1} - \frac{\mathbb{E}[(U_2 - \theta_2)]}{\theta_2} - \frac{\mathbb{E}[(U_2 - \theta_2)(U_1 - \theta_1)]}{\theta_2 \theta_1} + \frac{\mathbb{E}[(U_2 - \theta_2)^2]}{\theta_2^2} + o\left(\frac{1}{n}\right) \right) \quad (37)$$

We now make use of the following expressions:

$$\mathbb{E}[(U_1 - \theta_1)] = \mathbb{E}[(U_2 - \theta_2)] = 0 \quad (38)$$

$$\mathbb{E}[(U_2 - \theta_2)(U_1 - \theta_1)] = \text{Cov}(U_2, U_1) \quad (39)$$

$$\mathbb{E}[(U_2 - \theta_2)^2] = \text{Var}(U_2) \quad (40)$$

$$(41)$$

Using these expressions the expectation of r becomes:

$$\mathbb{E}[r] = R \left(1 - \frac{\text{Cov}(U_2, U_1)}{\theta_2 \theta_1} + \frac{\text{Var}(U_2)}{\theta_2^2} + o\left(\frac{1}{n}\right) \right) \quad (42)$$

Using Equation (35), the linearity of covariance and with $\text{Var}(aX) = a^2 \text{Var}(X)$ we obtain:

$$\text{Cov}(U_2, U_1), \text{Var}(U_2) \in \mathcal{O}\left(\frac{1}{n}\right) \implies \mathbb{E}[r] = R \left(1 + \mathcal{O}\left(\frac{1}{n}\right) \right). \quad (43)$$

□

C De-biasing of ratios of straight averages

Let X and Y be random variables and let μ_X and μ_Y be the means of their distributions, respectively. Consider the problem of finding an unbiased estimator for the ratio of means:

$$R = \frac{\mu_Y}{\mu_X}. \quad (44)$$

A first approach to estimate this ratio R is to compute the ratio of the sample means: Let $(X_1, Y_1), \dots, (X_n, Y_n)$ be pairs of i.i.d. random variables that are jointly distributed:

$$r = \hat{R} = \frac{\hat{\mu}_Y}{\hat{\mu}_X} = \frac{\frac{1}{n} \sum_{i=1}^n Y_i}{\frac{1}{n} \sum_{i=1}^n X_i} = \frac{\bar{Y}}{\bar{X}}. \quad (45)$$

This, however, is a biased estimator, which can be seen as follows (we follow [Tin, 1965, Ogliore et al., 2011] here):

$$r = \frac{\bar{Y}}{\bar{X}} = \frac{\mu_Y}{\mu_X} \left(\frac{\bar{Y}}{\mu_Y} \right) \left(\frac{\bar{X}}{\mu_X} \right)^{-1} = R \left(1 + \frac{\bar{Y} - \mu_Y}{\mu_Y} \right) \left(1 + \frac{\bar{X} - \mu_X}{\mu_X} \right)^{-1}. \quad (46)$$

This has now the form of a converging geometric series. Thus, if

$$\left| \frac{\bar{X} - \mu_X}{\mu_X} \right| < 1, \quad (47)$$

we can expand $\left(1 + \frac{\bar{X} - \mu_X}{\mu_X} \right)^{-1}$ in a geometric series, which is defined as:

$$\sum_{k=0}^{\infty} a b^k = a + ab + ab^2 + \dots = \frac{a}{1-b}. \quad (48)$$

In our case we can identify $a = R \left(1 + \frac{\bar{Y} - \mu_Y}{\mu_Y} \right)$ and $b = -\frac{\bar{X} - \mu_X}{\mu_X}$.

Thus, using the geometric series expansion, we can write:

$$\begin{aligned} r &= R \left(1 + \frac{\bar{Y} - \mu_Y}{\mu_Y} \right) \left(1 - \frac{(\bar{X} - \mu_X)}{\mu_X} + \frac{(\bar{X} - \mu_X)^2}{\mu_X^2} - \frac{(\bar{X} - \mu_X)^3}{\mu_X^3} + \frac{(\bar{X} - \mu_X)^4}{\mu_X^4} - \dots \right) \\ &= R \left(1 + \frac{(\bar{Y} - \mu_Y)}{\mu_Y} - \frac{(\bar{X} - \mu_X)}{\mu_X} - \frac{(\bar{X} - \mu_X)(\bar{Y} - \mu_Y)}{\mu_Y \mu_X} + \frac{(\bar{X} - \mu_X)^2}{\mu_X^2} \right. \\ &\quad \left. + \frac{(\bar{X} - \mu_X)^2(\bar{Y} - \mu_Y)}{\mu_X^2 \mu_Y} - \frac{(\bar{X} - \mu_X)^3}{\mu_X^3} - \frac{(\bar{X} - \mu_X)^3(\bar{Y} - \mu_Y)}{\mu_X^3 \mu_Y} + \frac{(\bar{X} - \mu_X)^4}{\mu_X^4} + \dots \right) \end{aligned} \quad (49)$$

$$(50)$$

Neglecting higher order terms Since \bar{X} and \bar{Y} are U-statistics, we make use of the asymptotic behaviour of U-statistics. If $\zeta_1 > 0$, a U-statistics U_n of order m obtained from a sample of n observations behaves as $n \rightarrow \infty$ like ([Shao, 2003]):

$$\sqrt{n}(U_n - \mathbb{E}[U_n]) \xrightarrow{d} N(0, m^2 \zeta_1). \quad (51)$$

As we seek an estimator that is unbiased up until order n^{-2} and since $\mathbb{E}[\bar{X}] = \mu_X$, we can neglect all terms of order 5 or higher since for $n \rightarrow \infty$:

$$(\bar{X} - \mu_X)^5 \in \mathcal{O}(n^{-2.5}) \quad (52)$$

$$(\bar{X} - \mu_X)^4(\bar{Y} - \mu_Y) \in \mathcal{O}(n^{-2.5}) \quad (53)$$

Therefore, we obtain:

$$\begin{aligned} r &\approx R \left(1 + \frac{(\bar{Y} - \mu_Y)}{\mu_Y} - \frac{(\bar{X} - \mu_X)}{\mu_X} - \frac{(\bar{X} - \mu_X)(\bar{Y} - \mu_Y)}{\mu_Y \mu_X} + \frac{(\bar{X} - \mu_X)^2}{\mu_X^2} \right. \\ &\quad \left. + \frac{(\bar{X} - \mu_X)^2(\bar{Y} - \mu_Y)}{\mu_X^2 \mu_Y} - \frac{(\bar{X} - \mu_X)^3}{\mu_X^3} - \frac{(\bar{X} - \mu_X)^3(\bar{Y} - \mu_Y)}{\mu_X^3 \mu_Y} + \frac{(\bar{X} - \mu_X)^4}{\mu_X^4} \right) \end{aligned} \quad (54)$$

Identities to compute the terms of the series expansion of r

$$\mathbb{E}[\bar{X} - \mu_X] = \mathbb{E}[\bar{Y} - \mu_Y] = 0 \quad (55)$$

$$\mathbb{E}[(\bar{X} - \mu_X)^2] = \text{Var}(\bar{X}) = \frac{1}{n} \text{Var}(X) \quad (56)$$

$$\mathbb{E}\left[(\bar{X} - \mu_X)(\bar{Y} - \mu_Y)\right] = \text{Cov}(\bar{X}, \bar{Y}) = \frac{1}{n} \text{Cov}(X, Y) \quad (57)$$

$$\mathbb{E}\left[(\bar{X} - \mu_X)^2(\bar{Y} - \mu_Y)\right] = \text{Cov}(\bar{X}^2, \bar{Y}) - 2\mu_X \text{Cov}(\bar{X}, \bar{Y}) \quad (58)$$

$$= \frac{1}{n^2} \left(\text{Cov}(X^2, Y) - 2\mu_X \text{Cov}(X, Y) \right) \quad (59)$$

$$\mathbb{E}\left[(\bar{X} - \mu_X)^3\right] = \text{Cov}(\bar{X}^2, \bar{X}) - 2\mu_X \text{Var}(\bar{X}) \quad (60)$$

$$= \frac{1}{n^2} \text{Cov}(X^2, X) - \frac{2}{n^2} \mu_X \text{Var}(X) \quad (61)$$

$$\mathbb{E}\left[(\bar{X} - \mu_X)^3(\bar{Y} - \mu_Y)\right] = \text{Cov}(\bar{X}^3, \bar{Y}) - 3\mu_X \text{Cov}(\bar{X}^2, \bar{Y}) + 3\mu_X^2 \text{Cov}(\bar{X}, \bar{Y}) \quad (62)$$

$$= \frac{3}{n^2} \text{Var}(X) \text{Cov}(X, Y) + \mathcal{O}(n^{-3}) \quad (63)$$

$$\mathbb{E}\left[(\bar{X} - \mu_X)^4\right] = \text{Cov}(\bar{X}^3, \bar{X}) - 3\mu_X \text{Cov}(\bar{X}^2, \bar{X}) + 3\mu_X^2 \text{Var}(\bar{X}) \quad (64)$$

$$= \frac{3}{n^2} \text{Var}(X)^2 + \mathcal{O}(n^{-3}) \quad (65)$$

Bias Using these expressions we can compute the expectation value of $r = \hat{R}$:

$$\begin{aligned} \mathbb{E}[r] \approx R & \left(1 + \frac{1}{n} \left(\frac{\text{Var}(X)}{\mu_X^2} - \frac{\text{Cov}(X, Y)}{\mu_X \mu_Y} \right) + \frac{1}{n^2} \left(\frac{(\text{Cov}(X^2, Y) - 2\mu_X \text{Cov}(X, Y))}{\mu_X^2 \mu_Y} \right. \right. \\ & \left. \left. - \frac{(\text{Cov}(X^2, X) - 2\mu_X \text{Var}(X))}{\mu_X^3} - \frac{3 \text{Var}(X) \text{Cov}(X, Y)}{\mu_X^3 \mu_Y} + \frac{3 \text{Var}(X)^2}{\mu_X^4} \right) \right) \end{aligned} \quad (66)$$

The bias or $r = \hat{R}$ is defined as:

$$\text{Bias}(r) = \mathbb{E}[r] - R \quad (67)$$

$$= R \left(\frac{1}{n} \left(\frac{\text{Var}(X)}{\mu_X^2} - \frac{\text{Cov}(X, Y)}{\mu_X \mu_Y} \right) + \frac{1}{n^2} \left(\frac{(\text{Cov}(X^2, Y) - 2\mu_X \text{Cov}(X, Y))}{\mu_X^2 \mu_Y} \right. \right. \quad (68)$$

$$\left. \left. - \frac{(\text{Cov}(X^2, X) - 2\mu_X \text{Var}(X))}{\mu_X^3} - \frac{3 \text{Var}(X) \text{Cov}(X, Y)}{\mu_X^3 \mu_Y} + \frac{3 \text{Var}(X)^2}{\mu_X^4} \right) \right) \quad (69)$$

Therefore an unbiased version of r is:

$$r_{\text{unbiased}} = r - R \left(\frac{1}{n} \left(\frac{\text{Var}(X)}{\mu_X^2} - \frac{\text{Cov}(X, Y)}{\mu_X \mu_Y} \right) + \frac{1}{n^2} \left(\frac{(\text{Cov}(X^2, Y) - 2\mu_X \text{Cov}(X, Y))}{\mu_X^2 \mu_Y} \right. \right. \quad (70)$$

$$\left. \left. - \frac{(\text{Cov}(X^2, X) - 2\mu_X \text{Var}(X))}{\mu_X^3} - \frac{3 \text{Var}(X) \text{Cov}(X, Y)}{\mu_X^3 \mu_Y} + \frac{3 \text{Var}(X)^2}{\mu_X^4} \right) \right) \quad (71)$$

A corrected version of the estimator $r = \hat{R}$ is consequently given by:

$$\begin{aligned} r_{\text{corr}} := r & \left(1 - \frac{1}{n} \left(\frac{\widehat{\text{Var}}(\bar{X})}{\widehat{\mu}_X^2} - \frac{\widehat{\text{Cov}}(\bar{X}, \bar{Y})}{\widehat{\mu}_X \widehat{\mu}_Y} \right) - \frac{1}{n^2} \left(\frac{(\widehat{\text{Cov}}(\bar{X}^2, \bar{Y}) - 2\widehat{\mu}_X \widehat{\text{Cov}}(\bar{X}, \bar{Y}))}{\widehat{\mu}_X^2 \widehat{\mu}_Y} \right. \right. \\ & \left. \left. - \frac{(\widehat{\text{Cov}}(\bar{X}^2, \bar{X}) - 2\widehat{\mu}_X \widehat{\text{Var}}(\bar{X}))}{\widehat{\mu}_X^3} - \frac{3\widehat{\text{Var}}(\bar{X})\widehat{\text{Cov}}(\bar{X}, \bar{Y})}{\widehat{\mu}_X^3 \widehat{\mu}_Y} + \frac{3\widehat{\text{Var}}(\bar{X})^2}{\widehat{\mu}_X^4} \right) \right) \end{aligned} \quad (72)$$

In the above equation we again encounter ratios of estimators which again might be biased. Since we want to achieve a second order de-biasing we have to again recurse on the terms that have a $\mathcal{O}\left(\frac{1}{n}\right)$ dependency. However, we do not have to recurse on the terms that have a $\mathcal{O}\left(\frac{1}{n^2}\right)$ dependency, since any recursion would increase the power of the n -dependency. Therefore a debiased estimator up to order $\mathcal{O}(n^2)$ is:

$$r_{corr} := r \left(1 - \frac{1}{n} (r_b^* - r_a^*) - \frac{1}{n^2} \left(\frac{(\widehat{\text{Cov}}(X^2, Y) - 2\widehat{\mu}_X \widehat{\text{Cov}}(X, Y))}{\widehat{\mu}_X^2 \widehat{\mu}_Y} - \frac{(\widehat{\text{Cov}}(X^2, X) - 2\widehat{\mu}_X \widehat{\text{Var}}(X))}{\widehat{\mu}_X^3} - \frac{3\widehat{\text{Var}}(X)\widehat{\text{Cov}}(X, Y)}{\widehat{\mu}_X^3 \widehat{\mu}_Y} + \frac{3\widehat{\text{Var}}(X)^2}{\widehat{\mu}_X^4} \right) \right) \quad (73)$$

where

$$r_a^* = \underbrace{\frac{\widehat{\text{Cov}}(X, Y)}{\widehat{\mu}_X \widehat{\mu}_Y}}_{=r_a} \left(1 + \frac{1}{(n-1)} \left(\frac{\widehat{\mu}_Y \widehat{\text{Cov}}(X^2, Y) + \widehat{\mu}_X \widehat{\text{Cov}}(Y^2, X)}{\widehat{\text{Cov}}(X, Y) \widehat{\mu}_X \widehat{\mu}_Y} - 4 \right) - \frac{1}{(n-1)} \left(\frac{\widehat{\text{Var}}(X)}{\widehat{\mu}_X^2} + \frac{\widehat{\text{Var}}(Y)}{\widehat{\mu}_Y^2} + 2 \frac{\widehat{\text{Cov}}(X, Y)}{\widehat{\mu}_X \widehat{\mu}_Y} \right) \right) \quad (74)$$

$$r_b^* = \underbrace{\frac{\widehat{\text{Var}}(X)}{\widehat{\mu}_X^2}}_{=r_b} \left(1 + \frac{4}{(n-1)} \left(\frac{\frac{1}{2} \widehat{\text{Cov}}(X^2, X)}{\widehat{\mu}_X \widehat{\text{Var}}(X)} - 1 \right) - \frac{4}{(n-1)} \frac{\widehat{\text{Var}}(X)}{\widehat{\mu}_X^2} \right). \quad (75)$$

D De-biasing of ratios of squared means

Now consider the problem of finding an unbiased estimator for the ratio of the squared means of x and Y :

$$R = \frac{\mu_Y^2}{\mu_X^2}. \quad (76)$$

Both the numerator and denominator of R can separately be estimated by a second order U-statistics, respectively:

$$r = \hat{R} = \frac{\widehat{\mu}_Y^2}{\widehat{\mu}_X^2} = \frac{\frac{1}{n(n-1)} \sum_{i=1}^n \sum_{j=1 \wedge j \neq i}^n Y_i Y_j}{\frac{1}{n(n-1)} \sum_{i=1}^n \sum_{j=1 \wedge j \neq i}^n X_i X_j} =: \frac{\bar{Y}_2}{\bar{X}_2}. \quad (77)$$

The subscript 2 in \bar{X}_2 should emphasize that we are dealing with a second order U-statistics here. Again, the ratio $\frac{\bar{Y}_2}{\bar{X}_2}$ is a biased estimator. Using the approach with the converging geometric series and neglecting the higher order terms, we obtain:

$$r \approx R \left(1 + \frac{(\bar{Y}_2 - \mu_Y^2)}{\mu_Y^2} - \frac{(\bar{X}_2 - \mu_X^2)}{\mu_X^2} - \frac{(\bar{X}_2 - \mu_X^2)(\bar{Y}_2 - \mu_Y^2)}{\mu_Y^2 \mu_X^2} + \frac{(\bar{X}_2 - \mu_X^2)^2}{\mu_X^4} + \frac{(\bar{X}_2 - \mu_X^2)^2 (\bar{Y}_2 - \mu_Y^2)}{\mu_X^4 \mu_Y^2} - \frac{(\bar{X}_2 - \mu_X^2)^3}{\mu_X^6} - \frac{(\bar{X}_2 - \mu_X^2)^3 (\bar{Y}_2 - \mu_Y^2)}{\mu_X^6 \mu_Y^2} + \frac{(\bar{X}_2 - \mu_X^2)^4}{\mu_X^8} \right) \quad (78)$$

Identities to compute the terms of the series expansion of r

$$\mathbb{E}[\bar{X}_2 - \mu_X^2] = \mathbb{E}[\bar{Y}_2 - \mu_Y^2] = 0 \quad (79)$$

$$\mathbb{E}[(\bar{X}_2 - \mu_X^2)^2] = \text{Var}(\bar{X}_2) \quad (80)$$

$$\mathbb{E}\left[(\bar{X}_2 - \mu_X^2)(\bar{Y}_2 - \mu_Y^2)\right] = \text{Cov}(\bar{X}_2, \bar{Y}_2) \quad (81)$$

$$\mathbb{E}\left[(\bar{X}_2 - \mu_X^2)^2(\bar{Y}_2 - \mu_Y^2)\right] = \text{Cov}(\bar{X}_2^2, \bar{Y}_2) - 2\mu_X^2 \text{Cov}(\bar{X}_2, \bar{Y}_2) \quad (82)$$

$$\mathbb{E}\left[(\bar{X}_2 - \mu_X^2)^3\right] = \text{Cov}(\bar{X}_2^2, \bar{X}_2) - 2\mu_X^2 \text{Var}(\bar{X}_2) \quad (83)$$

$$\mathbb{E}\left[(\bar{X}_2 - \mu_X^2)^3(\bar{Y}_2 - \mu_Y^2)\right] = \text{Cov}(\bar{X}_2^3, \bar{Y}_2) - 3\mu_X^2 \text{Cov}(\bar{X}_2^2, \bar{Y}_2) + 3\mu_X^4 \text{Cov}(\bar{X}_2, \bar{Y}_2) \quad (84)$$

$$\mathbb{E}\left[(\bar{X}_2 - \mu_X^2)^4\right] = \text{Cov}(\bar{X}_2^3, \bar{X}_2) - 3\mu_X^2 \text{Cov}(\bar{X}_2^2, \bar{X}_2) + 3\mu_X^4 \text{Var}(\bar{X}_2) \quad (85)$$

Bias Computing $\mathbb{E}[r]$ using the above identities:

$$\begin{aligned} \mathbb{E}[r] \approx R & \left(1 - \frac{\text{Cov}(\bar{X}_2, \bar{Y}_2)}{\mu_X^2 \mu_Y^2} + \frac{\text{Var}(\bar{X}_2)}{\mu_X^4} + \left(\frac{\text{Cov}(\bar{X}_2^2, \bar{Y}_2) - 2\mu_X^2 \text{Cov}(\bar{X}_2, \bar{Y}_2)}{\mu_X^4 \mu_Y^2} \right) \right. \\ & - \left(\frac{\text{Cov}(\bar{X}_2^2, \bar{X}_2) - 2\mu_X^2 \text{Var}(\bar{X}_2)}{\mu_X^6} \right) - \left(\frac{\text{Cov}(\bar{X}_2^3, \bar{Y}_2) - 3\mu_X^2 \text{Cov}(\bar{X}_2^2, \bar{Y}_2) + 3\mu_X^4 \text{Cov}(\bar{X}_2, \bar{Y}_2)}{\mu_X^6 \mu_Y^2} \right) \\ & \left. + \left(\frac{\text{Cov}(\bar{X}_2^3, \bar{X}_2) - 3\mu_X^2 \text{Cov}(\bar{X}_2^2, \bar{X}_2) + 3\mu_X^4 \text{Var}(\bar{X}_2)}{\mu_X^8} \right) \right) \end{aligned} \quad (86)$$

$$\begin{aligned} = R & \left(1 - \underbrace{\frac{6 \text{Cov}(\bar{X}_2, \bar{Y}_2)}{\mu_X^2 \mu_Y^2}}_{\text{Term (a)}} + \underbrace{\frac{6 \text{Var}(\bar{X}_2)}{\mu_X^4}}_{\text{Term (b)}} + \underbrace{\frac{4 \text{Cov}(\bar{X}_2^2, \bar{Y}_2)}{\mu_X^4 \mu_Y^2}}_{\text{Term (c)}} - \underbrace{\frac{4 \text{Cov}(\bar{X}_2^2, \bar{X}_2)}{\mu_X^6}}_{\text{Term (d)}} \right. \\ & \left. - \underbrace{\frac{\text{Cov}(\bar{X}_2^3, \bar{Y}_2)}{\mu_X^6 \mu_Y^2}}_{\text{Term (e)}} + \underbrace{\frac{\text{Cov}(\bar{X}_2^3, \bar{X}_2)}{\mu_X^8}}_{\text{Term (f)}} \right) \end{aligned} \quad (87)$$

$$\begin{aligned}
&= R \left\{ 1 - \left(\frac{12}{n(n-1)} \frac{\text{Cov}(X, Y)^2}{\mu_X^2 \mu_Y^2} + \frac{24}{n} R_a \right) \right. \\
&\quad + \left(\frac{12}{n(n-1)} \frac{\text{Var}(X)^2}{\mu_X^4} + \frac{24}{n} R_b \right) \\
&\quad + \left(\frac{32(n-2)}{n(n-1)^2} \left(\frac{\text{Cov}(X^2, Y)}{\mu_X^2 \mu_Y} + \frac{2 \text{Cov}(X, Y)(\text{Var}(X) + \mu_X^2)}{\mu_X^3 \mu_Y} \right) \right. \\
&\quad \left. + \frac{4(n-2)(n-3)}{n(n-1)} \left(\frac{8}{n} R_a + \frac{12}{n(n-1)} \frac{\text{Cov}(X, Y)^2}{\mu_X^2 \mu_Y^2} \right) \right) \\
&\quad - \left(\frac{32(n-2)}{n(n-1)^2} \left(\frac{\text{Cov}(X^2, X)}{\mu_X^3} + \frac{2 \text{Var}(X)(\text{Var}(X) + \mu_X^2)}{\mu_X^4} \right) \right. \\
&\quad \left. + \frac{4(n-2)(n-3)}{n(n-1)} \left(\frac{8}{n} R_b + \frac{12}{n(n-1)} \frac{\text{Var}(X)^2}{\mu_X^4} \right) \right) \\
&\quad - \left(\frac{24(n-2)(n-3)(n-4)}{n^2(n-1)^3} \left(\frac{\text{Cov}(X^2, Y)}{\mu_Y \mu_X^2} + \frac{4 \text{Cov}(X, Y)(\text{Var}(X) + \mu_X^2)}{\mu_Y \mu_X^3} \right) \right. \\
&\quad \left. + \frac{(n-2)(n-3)(n-4)(n-5)}{n^2(n-1)^2} \left(\frac{12}{n} R_a + \frac{30}{n(n-1)} \frac{\text{Cov}(X, Y)^2}{\mu_X^2 \mu_Y^2} \right) \right) \\
&\quad + \left(\frac{24(n-2)(n-3)(n-4)}{n^2(n-1)^3} \left(\frac{\text{Cov}(X^2, X)}{\mu_X^3} + \frac{4 \text{Var}(X)(\text{Var}(X) + \mu_X^2)}{\mu_X^4} \right) \right. \\
&\quad \left. + \frac{(n-2)(n-3)(n-4)(n-5)}{n^2(n-1)^2} \left(\frac{12}{n} R_b + \frac{30}{n(n-1)} \frac{\text{Var}(X)^2}{\mu_X^4} \right) \right) \\
&\quad \left. \right\} \tag{88}
\end{aligned}$$

where $R_a = \frac{\text{Cov}(X, Y)}{\mu_X \mu_Y}$ and $R_b = \frac{\text{Var}(X)}{\mu_X^2}$ and where we have used 97, 101 110, 111, 124 and 126 for terms (a)-(f).

Therefore, an estimator unbiased up to order two is given by:

$$\begin{aligned}
r_{\text{corr}} = \frac{\widehat{\mu_Y^2}}{\widehat{\mu_X^2}} & \left\{ 1 + \left(\frac{12}{n(n-1)} \frac{\widehat{\text{Cov}(X, Y)^2}}{\widehat{\mu_X^2} \widehat{\mu_Y^2}} + \frac{24}{n} r_a^* \right) \right. \\
& - \left(\frac{12}{n(n-1)} \frac{\widehat{\text{Var}(X)^2}}{\widehat{\mu_X^4}} + \frac{24}{n} r_b^* \right) \\
& - \left(\frac{32(n-2)}{n(n-1)^2} \left(\frac{\widehat{\text{Cov}(X^2, Y)}}{\widehat{\mu_X^2} \widehat{\mu_Y}} + \frac{2\widehat{\text{Cov}(X, Y)}(\widehat{\text{Var}(X)} + \widehat{\mu_X^2})}{\widehat{\mu_X^3} \widehat{\mu_Y}} \right) \right. \\
& \quad \left. + \frac{4(n-2)(n-3)}{n(n-1)} \left(\frac{8}{n} r_a^* + \frac{12}{n(n-1)} \frac{\widehat{\text{Cov}(X, Y)^2}}{\widehat{\mu_X^2} \widehat{\mu_Y^2}} \right) \right) \\
& + \left(\frac{32(n-2)}{n(n-1)^2} \left(\frac{\widehat{\text{Cov}(X^2, X)}}{\widehat{\mu_X^3}} + \frac{2\widehat{\text{Var}(X)}(\widehat{\text{Var}(X)} + \widehat{\mu_X^2})}{\widehat{\mu_X^4}} \right) \right. \\
& \quad \left. + \frac{4(n-2)(n-3)}{n(n-1)} \left(\frac{8}{n} r_b^* + \frac{12}{n(n-1)} \frac{\widehat{\text{Var}(X)^2}}{\widehat{\mu_X^4}} \right) \right) \\
& + \left(\frac{24(n-2)(n-3)(n-4)}{n^2(n-1)^3} \left(\frac{\widehat{\text{Cov}(X^2, Y)}}{\widehat{\mu_Y} \widehat{\mu_X^2}} + \frac{4\widehat{\text{Cov}(X, Y)}(\widehat{\text{Var}(X)} + \widehat{\mu_X^2})}{\widehat{\mu_Y} \widehat{\mu_X^3}} \right) \right. \\
& \quad \left. + \frac{(n-2)(n-3)(n-4)(n-5)}{n^2(n-1)^2} \left(\frac{12}{n} r_a^* + \frac{30}{n(n-1)} \frac{\widehat{\text{Cov}(X, Y)^2}}{\widehat{\mu_X^2} \widehat{\mu_Y^2}} \right) \right) \\
& - \left(\frac{24(n-2)(n-3)(n-4)}{n^2(n-1)^3} \left(\frac{\widehat{\text{Cov}(X^2, X)}}{\widehat{\mu_X^3}} + \frac{4\widehat{\text{Var}(X)}(\widehat{\text{Var}(X)} + \widehat{\mu_X^2})}{\widehat{\mu_X^4}} \right) \right. \\
& \quad \left. + \frac{(n-2)(n-3)(n-4)(n-5)}{n^2(n-1)^2} \left(\frac{12}{n} r_b^* + \frac{30}{n(n-1)} \frac{\widehat{\text{Var}(X)^2}}{\widehat{\mu_X^4}} \right) \right), \tag{89}
\end{aligned}$$

where we used equations (96), (100):

$$r_a^* = \underbrace{\frac{\widehat{\text{Cov}(X, Y)}}{\widehat{\mu_X} \widehat{\mu_Y}}}_{=r_a} \left(1 + \frac{1}{(n-1)} \left(\frac{\widehat{\mu_Y} \widehat{\text{Cov}(X^2, Y)} + \widehat{\mu_X} \widehat{\text{Cov}(Y^2, X)}}{\widehat{\text{Cov}(X, Y)} \widehat{\mu_X} \widehat{\mu_Y}} - 4 \right) \right. \tag{90}$$

$$\left. - \frac{1}{(n-1)} \left(\frac{\widehat{\text{Var}(X)}}{\widehat{\mu_X^2}} + \frac{\widehat{\text{Var}(Y)}}{\widehat{\mu_Y^2}} + 2 \frac{\widehat{\text{Cov}(X, Y)}}{\widehat{\mu_X} \widehat{\mu_Y}} \right) \right)$$

$$r_b^* = \underbrace{\frac{\widehat{\text{Var}(X)}}{\widehat{\mu_X^2}}}_{=r_b} \left(1 + \frac{4}{(n-1)} \left(\frac{\frac{1}{2} \widehat{\text{Cov}(X^2, X)}}{\widehat{\mu_X} \widehat{\text{Var}(X)}} - 1 \right) - \frac{4}{(n-1)} \frac{\widehat{\text{Var}(X)}}{\widehat{\mu_X^2}} \right). \tag{91}$$

D.1 Term (a)

Let us first look at the first term: $\frac{6 \text{Cov}(\bar{X}_2, \bar{Y}_2)}{\mu_X^2 \mu_Y^2}$. Using the expression for the covariance between two second order U-statistics we get:

$$\frac{6 \text{Cov}(\bar{X}_2, \bar{Y}_2)}{\mu_X^2 \mu_Y^2} = \frac{6}{\mu_X^2 \mu_Y^2} \left(\frac{4}{n} \mu_X \mu_Y \text{Cov}(X, Y) + \frac{2}{n(n-1)} \text{Cov}(X, Y)^2 \right) \tag{92}$$

$$= \underbrace{\frac{24 \text{Cov}(X, Y)}{n \mu_X \mu_Y}}_{\in \mathcal{O}(n^{-1})} + \underbrace{\frac{12 \text{Cov}(X, Y)^2}{n(n-1) \mu_X^2 \mu_Y^2}}_{\in \mathcal{O}(n^{-2})} \tag{93}$$

Since we know that for every recursion (i.e., geometric series expansion) we will get at least another factor of $\frac{1}{n}$, we don't have to further recurse on term that is of order $\mathcal{O}(n^{-2})$. Consequently, we only expand the following term via a geometric series,

$$R_a = \frac{\text{Cov}(X, Y)}{\mu_X \mu_Y}, \quad (94)$$

since the ratio of the respective unbiased estimators,

$$r_a = \frac{\widehat{\text{Cov}}(X, Y)}{\widehat{\mu}_X \widehat{\mu}_Y}, \quad (95)$$

is biased.

Using the same machinery as before, we obtain a corrected version of r_a :

$$r_a^* = \underbrace{\frac{\widehat{\text{Cov}}(X, Y)}{\widehat{\mu}_X \widehat{\mu}_Y}}_{=r_a} \left(1 + \frac{1}{(n-1)} \left(\frac{\widehat{\mu}_Y \widehat{\text{Cov}}(X^2, Y) + \widehat{\mu}_X \widehat{\text{Cov}}(Y^2, X)}{\widehat{\text{Cov}}(X, Y) \widehat{\mu}_X \widehat{\mu}_Y} - 4 \right) - \frac{1}{(n-1)} \left(\frac{\widehat{\text{Var}}(X)}{\widehat{\mu}_X^2} + \frac{\widehat{\text{Var}}(Y)}{\widehat{\mu}_Y^2} + 2 \frac{\widehat{\text{Cov}}(X, Y)}{\widehat{\mu}_X \widehat{\mu}_Y} \right) \right) \quad (96)$$

The complete correction of term (a), $\frac{6 \widehat{\text{Cov}}(\bar{X}_2, \bar{Y}_2)}{\widehat{\mu}_X^2 \widehat{\mu}_Y^2}$, looks therefore as follows:

$$\begin{aligned} \frac{6 \widehat{\text{Cov}}(\bar{X}_2, \bar{Y}_2)}{\widehat{\mu}_X^2 \widehat{\mu}_Y^2} &= \frac{12}{n(n-1)} \frac{\widehat{\text{Cov}}(X, Y)^2}{\widehat{\mu}_X^2 \widehat{\mu}_Y^2} \\ &+ \frac{24}{n} \frac{\widehat{\text{Cov}}(X, Y)}{\widehat{\mu}_X \widehat{\mu}_Y} \left(1 + \frac{1}{(n-1)} \left(\frac{\widehat{\mu}_Y \widehat{\text{Cov}}(X^2, Y) + \widehat{\mu}_X \widehat{\text{Cov}}(Y^2, X)}{\widehat{\text{Cov}}(X, Y) \widehat{\mu}_X \widehat{\mu}_Y} - 4 \right) - \frac{1}{(n-1)} \left(\frac{\widehat{\text{Var}}(X)}{\widehat{\mu}_X^2} + \frac{\widehat{\text{Var}}(Y)}{\widehat{\mu}_Y^2} + 2 \frac{\widehat{\text{Cov}}(X, Y)}{\widehat{\mu}_X \widehat{\mu}_Y} \right) \right) \end{aligned} \quad (97)$$

D.2 Term (b)

The correction of term (b), $\frac{6 \widehat{\text{Var}}(\bar{X}_2)}{\widehat{\mu}_X^4}$ is analogous to that of term (a). Define

$$R_b = \frac{\widehat{\text{Var}}(X)}{\widehat{\mu}_X^2} \quad (98)$$

$$r_b = \frac{\widehat{\text{Var}}(X)}{\widehat{\mu}_X^2}. \quad (99)$$

Then using the geometric series expansion, a corrected version of r_b is given by

$$r_b^* = \underbrace{\frac{\widehat{\text{Var}}(X)}{\widehat{\mu}_X^2}}_{=r_b} \left(1 + \frac{4}{(n-1)} \left(\frac{\frac{1}{2} \widehat{\text{Cov}}(X^2, X)}{\widehat{\mu}_X \widehat{\text{Var}}(X)} - 1 \right) - \frac{4}{(n-1)} \frac{\widehat{\text{Var}}(X)}{\widehat{\mu}_X^2} \right). \quad (100)$$

The full correction of term (b) is

$$\frac{6 \widehat{\text{Var}}(\bar{X}_2)}{\widehat{\mu}_X^4} = \frac{12}{n(n-1)} \frac{\widehat{\text{Var}}(X)^2}{\widehat{\mu}_X^4} + \frac{24}{n} \frac{\widehat{\text{Var}}(X)}{\widehat{\mu}_X^2} \left(1 + \frac{4}{(n-1)} \left(\frac{\frac{1}{2} \widehat{\text{Cov}}(X^2, X)}{\widehat{\mu}_X \widehat{\text{Var}}(X)} - 1 - \frac{\widehat{\text{Var}}(X)}{\widehat{\mu}_X^2} \right) \right) \quad (101)$$

D.3 Term (c)

In this section we want to find an expression for term (c):

$$\frac{4 \text{Cov}(\bar{X}_2^2, \bar{Y}_2)}{\mu_X^4 \mu_Y^2}. \quad (102)$$

To this end, we first need a convenient representation of \bar{X}_2^2 in terms of other U-statistics:

$$\bar{X}_2^2 = \left(\frac{1}{n(n-1)} \sum_{i=1}^n \sum_{\substack{j=1 \\ j \neq i}}^n X_i X_j \right)^2 = \frac{2}{n(n-1)} U_\alpha + \frac{4(n-2)}{n(n-1)} U_\beta + \frac{(n-2)(n-3)}{n(n-1)} \bar{X}_4, \quad (103)$$

with the U-statistics:

$$U_\beta = \frac{1}{n(n-1)(n-2)} \sum_{i=1}^n \sum_{\substack{j=1 \\ j \neq i}}^n \sum_{\substack{k=1 \\ k \neq j \\ k \neq i}}^n X_i^2 X_j X_k \quad (104)$$

$$U_\alpha = \frac{1}{n(n-1)} \sum_{i=1}^n \sum_{\substack{j=1 \\ j \neq i}}^n X_i^2 X_j^2 \quad (105)$$

$$\bar{X}_4 = \frac{1}{n(n-1)(n-2)(n-3)} \sum_{i=1}^n \sum_{\substack{j=1 \\ j \neq i}}^n \sum_{\substack{k=1 \\ k \neq j \\ k \neq i}}^n \sum_{\substack{l=1 \\ l \neq k \\ l \neq j \\ l \neq i}}^n X_i X_j X_k X_l. \quad (106)$$

Hence, term (c) becomes:

$$\frac{4 \text{Cov}(\bar{X}_2^2, \bar{Y}_2)}{\mu_X^4 \mu_Y^2} = \underbrace{\frac{8}{n(n-1)} \frac{\text{Cov}(U_\alpha, \bar{Y}_2)}{\mu_X^4 \mu_Y^2}}_{\text{First term}} + \underbrace{\frac{16(n-2)}{n(n-1)} \frac{\text{Cov}(U_\beta, \bar{Y}_2)}{\mu_X^4 \mu_Y^2}}_{\text{Second term}} + \underbrace{\frac{4(n-2)(n-3)}{n(n-1)} \frac{\text{Cov}(\bar{X}_4, \bar{Y}_2)}{\mu_X^4 \mu_Y^2}}_{\text{Third term}} \quad (107)$$

All all the covariances in the above equation are covariances between U-statistics which are $\mathcal{O}(\frac{1}{n})$. Therefore, the first term, which already has an explicit $\mathcal{O}(\frac{1}{n^2})$ dependence, can be neglected entirely. The second term has an explicit $\mathcal{O}(\frac{1}{n})$, combined with the $\mathcal{O}(\frac{1}{n})$ from the covariance this is in total a $\mathcal{O}(\frac{1}{n^2})$ dependency. Hence, we have to find an estimator for that term but do not have to recurse on it. On the last term, we do have to recurse, however, we have derived the recursion already in equation (96). We can rewrite the above equation using the symmetrized U-statistics

$$U_\beta = \frac{1}{n(n-1)(n-2)} \sum_{i=1}^n \sum_{\substack{j=1 \\ j \neq i}}^n \sum_{\substack{k=1 \\ k \neq j \\ k \neq i}}^n \frac{1}{3} (X_i^2 X_j X_k + X_i X_j^2 X_k + X_i X_j X_k^2). \quad (108)$$

$$\begin{aligned} \frac{4 \text{Cov}(\bar{X}_2^2, \bar{Y}_2)}{\mu_X^4 \mu_Y^2} &\approx \underbrace{\frac{32(n-2)}{n(n-1)^2} \left(\frac{\text{Cov}(X^2, Y)}{\mu_X^2 \mu_Y} + \frac{2 \text{Cov}(X, Y)(\text{Var}(X) + \mu_X^2)}{\mu_X^3 \mu_Y} \right)}_{\text{Second term}} \\ &+ \underbrace{\frac{4(n-2)(n-3)}{n(n-1)} \left(\frac{8 \text{Cov}(X, Y)}{n \mu_X \mu_Y} + \frac{12}{n(n-1)} \frac{\text{Cov}(X, Y)^2}{\mu_X^2 \mu_Y^2} \right)}_{\text{Third term}} \end{aligned} \quad (109)$$

Taking the recursion of the third term into account, the total correction of term (c) is:

$$\begin{aligned} \frac{4 \text{Cov}(\widehat{\bar{X}}_2^2, \widehat{\bar{Y}}_2)}{\widehat{\mu}_X^4 \widehat{\mu}_Y^2} &\approx \frac{32(n-2)}{n(n-1)^2} \left(\frac{\widehat{\text{Cov}}(X^2, Y)}{\widehat{\mu}_X^2 \widehat{\mu}_Y} + \frac{2 \widehat{\text{Cov}}(X, Y)(\widehat{\text{Var}}(X) + \widehat{\mu}_X^2)}{\widehat{\mu}_X^3 \widehat{\mu}_Y} \right) \\ &+ \frac{4(n-2)(n-3)}{n(n-1)} \left(\frac{8}{n} r_a^* + \frac{12}{n(n-1)} \frac{\widehat{\text{Cov}}(X, Y)^2}{\widehat{\mu}_X^2 \widehat{\mu}_Y^2} \right) \end{aligned} \quad (110)$$

D.4 Term (d)

The computation of the correction of term (d), $\frac{4 \text{Cov}(\bar{X}_2^2, \bar{X}_2)}{\mu_X^6}$, is similar to that of term (c). Hence, we only present the resulting correction:

$$\begin{aligned} \frac{4 \text{Cov}(\widehat{\bar{X}_2^2}, \widehat{\bar{X}_2})}{\widehat{\mu_X^4} \widehat{\mu_Y^2}} &\approx \frac{32(n-2)}{n(n-1)^2} \left(\frac{\text{Cov}(\widehat{X^2}, X)}{\widehat{\mu_X^3}} + \frac{2 \widehat{\text{Var}}(X)(\widehat{\text{Var}}(X) + \widehat{\mu_X^2})}{\widehat{\mu_X^4}} \right) \\ &+ \frac{4(n-2)(n-3)}{n(n-1)} \left(\frac{8}{n} r_b^* + \frac{12}{n(n-1)} \frac{\widehat{\text{Var}}(X)^2}{\widehat{\mu_X^4}} \right) \end{aligned} \quad (111)$$

D.5 Term (e)

Term (e) is:

$$\frac{\text{Cov}(\bar{X}_2^3, \bar{Y}_2)}{\mu_X^6 \mu_Y^2} \quad (112)$$

To be able to compute that term, we reexpress the numerator in terms of several U-statistics:

$$\begin{aligned} \bar{X}_2^3 &= \frac{4}{n^2(n-1)^2} U_I + \frac{24(n-2)}{n^2(n-1)^2} U_{II} + \frac{8(n-2)}{n^2(n-1)^2} U_{III} + \frac{8(n-2)(n-3)}{n^2(n-1)^2} U_{IV} \\ &+ \frac{30(n-2)(n-3)}{n^2(n-1)^2} U_V + \frac{12(n-2)(n-3)(n-4)}{n^2(n-1)^2} U_{VI} + \frac{(n-2)(n-2)(n-4)(n-5)}{n^2(n-1)^2} \bar{X}_6, \end{aligned} \quad (113)$$

where

$$U_I := \frac{1}{n(n-1)} \sum_{i=1}^n \sum_{\substack{j=1 \\ j \neq i}}^n X_i^3 X_j^3, \quad (114)$$

$$U_{II} := \frac{1}{n(n-1)(n-2)} \sum_{i=1}^n \sum_{\substack{j=1 \\ j \neq i}}^n \sum_{\substack{k=1 \\ k \neq j \\ k \neq i}}^n X_i^3 X_j^2 X_k, \quad (115)$$

$$U_{III} = \frac{1}{n(n-1)(n-2)} \sum_{i=1}^n \sum_{\substack{j=1 \\ j \neq i}}^n \sum_{\substack{k=1 \\ k \neq j \\ k \neq i}}^n X_i^2 X_j^2 X_k^2 \quad (116)$$

$$U_{IV} := \frac{1}{n(n-1)(n-2)(n-3)} \sum_{i=1}^n \sum_{\substack{j=1 \\ j \neq i}}^n \sum_{\substack{k=1 \\ k \neq j \\ k \neq i}}^n \sum_{\substack{l=1 \\ l \neq k \\ l \neq j \\ l \neq i}}^n X_i^3 X_j X_k X_l, \quad (117)$$

$$U_V := \frac{1}{n(n-1)(n-2)(n-3)} \sum_{i=1}^n \sum_{\substack{j=1 \\ j \neq i}}^n \sum_{\substack{k=1 \\ k \neq j \\ k \neq i}}^n \sum_{\substack{l=1 \\ l \neq k \\ l \neq j \\ l \neq i}}^n X_i^2 X_j^2 X_k X_l, \quad (118)$$

$$U_{VI} := \frac{1}{n(n-1)(n-2)(n-3)(n-4)} \sum_{i=1}^n \sum_{\substack{j=1 \\ j \neq i}}^n \sum_{\substack{k=1 \\ k \neq j \\ k \neq i}}^n \sum_{\substack{l=1 \\ l \neq k \\ l \neq j \\ l \neq i}}^n \sum_{\substack{p=1 \\ p \neq l \\ p \neq k \\ p \neq j \\ p \neq i}}^n X_i^2 X_j X_k X_l X_p, \quad (119)$$

$$\bar{X}_6 = \frac{1}{n(n-1)(n-2)(n-3)(n-4)(n-5)} \sum_{i=1}^n \sum_{\substack{j=1 \\ j \neq i}}^n \sum_{\substack{k=1 \\ k \neq j \\ k \neq i}}^n \sum_{\substack{l=1 \\ l \neq k \\ l \neq j \\ l \neq i}}^n \sum_{\substack{p=1 \\ p \neq l \\ p \neq k \\ p \neq j \\ p \neq i}}^n \sum_{\substack{q=1 \\ q \neq p \\ q \neq k \\ q \neq j \\ q \neq i}}^n X_i X_j X_k X_l X_p X_q, \quad (120)$$

Hence term (e) can be written as:

$$\begin{aligned} \frac{\text{Cov}(\bar{X}_2^3, \bar{Y}_2)}{\mu_X^6 \mu_Y^2} &= \underbrace{\frac{4}{n^2(n-1)^2} \frac{\text{Cov}(U_I, \bar{Y}_2)}{\mu_X^6 \mu_Y^2}}_{\in \mathcal{O}(\frac{1}{n^4})} + \underbrace{\frac{24(n-2)}{n^2(n-1)^2} \frac{\text{Cov}(U_{II}, \bar{Y}_2)}{\mu_X^6 \mu_Y^2}}_{\in \mathcal{O}(\frac{1}{n^3})} + \underbrace{\frac{8(n-2)}{n^2(n-1)^2} \frac{\text{Cov}(U_{III}, \bar{Y}_2)}{\mu_X^6 \mu_Y^2}}_{\in \mathcal{O}(\frac{1}{n^3})} \\ &+ \underbrace{\frac{8(n-2)(n-3)}{n^2(n-1)^2} \frac{\text{Cov}(U_{IV}, \bar{Y}_2)}{\mu_X^6 \mu_Y^2}}_{\in \mathcal{O}(\frac{1}{n^2})} + \underbrace{\frac{30(n-2)(n-3)}{n^2(n-1)^2} \frac{\text{Cov}(U_V, \bar{Y}_2)}{\mu_X^6 \mu_Y^2}}_{\in \mathcal{O}(\frac{1}{n^2})} \\ &+ \underbrace{\frac{12(n-2)(n-3)(n-4)}{n^2(n-1)^2} \frac{\text{Cov}(U_{VI}, \bar{Y}_2)}{\mu_X^6 \mu_Y^2}}_{\in \mathcal{O}(\frac{1}{n})} + \underbrace{\frac{(n-2)(n-3)(n-4)(n-5)}{n^2(n-1)^2} \frac{\text{Cov}(\bar{X}_6, \bar{Y}_2)}{\mu_X^6 \mu_Y^2}}_{\in \mathcal{O}(1)}. \end{aligned} \quad (121)$$

At this point, we can immediately discard the first three terms as they are at least $\mathcal{O}(\frac{1}{n^3})$ and so can directly be neglected for a second order correction. In addition, as we are dealing with covariances between U-statistics they add another $\mathcal{O}(\frac{1}{n})$. Therefore, the fourth and fifth term are actually $\mathcal{O}(\frac{1}{n}) \mathcal{O}(\frac{1}{n^2}) = \mathcal{O}(\frac{1}{n^3})$, so they can be neglected as well. Only the last and the second to last term remain:

$$\frac{\text{Cov}(\bar{X}_2^3, \bar{Y}_2)}{\mu_X^6 \mu_Y^2} \approx \underbrace{\frac{12(n-2)(n-3)(n-4)}{n^2(n-1)^2} \frac{\text{Cov}(U_{VI}, \bar{Y}_2)}{\mu_X^6 \mu_Y^2}}_{\text{Sixth term}} + \underbrace{\frac{(n-2)(n-3)(n-4)(n-5)}{n^2(n-1)^2} \frac{\text{Cov}(\bar{X}_6, \bar{Y}_2)}{\mu_X^6 \mu_Y^2}}_{\text{Seventh term}}. \quad (122)$$

Re-expressing the covariances between U-statistics as covariances between random variables X and Y (and using the symmetrized version of U_{VI}), we obtain:

$$\begin{aligned} \frac{\text{Cov}(\bar{X}_2^3, \bar{Y}_2)}{\mu_X^6 \mu_Y^2} &\approx \underbrace{\frac{24(n-2)(n-3)(n-4)}{n^2(n-1)^3} \left(\frac{\text{Cov}(X^2, Y)}{\mu_Y \mu_X^2} + \frac{4 \text{Cov}(X, Y)(\text{Var}(X) + \mu_X^2)}{\mu_Y \mu_X^3} \right)}_{\text{Sixth term}} \\ &+ \underbrace{\frac{(n-2)(n-3)(n-4)(n-5)}{n^2(n-1)^2} \left(\frac{12}{n} \frac{\text{Cov}(X, Y)}{\mu_X \mu_Y} + \frac{30}{n(n-1)} \frac{\text{Cov}(X, Y)^2}{\mu_X^2 \mu_Y^2} \right)}_{\text{Seventh term}} \end{aligned} \quad (123)$$

Since the term $\frac{12}{n} \frac{\text{Cov}(X, Y)}{\mu_X \mu_Y}$ is in $\mathcal{O}(\frac{1}{n})$ we have to recurse on it. However, we already have derived its correction in equation (96). Therefore, the total correction of term (e) comes down to:

$$\begin{aligned} \frac{\widehat{\text{Cov}}(\bar{X}_2^3, \bar{Y}_2)}{\widehat{\mu}_X^6 \widehat{\mu}_Y^2} &= \frac{24(n-2)(n-3)(n-4)}{n^2(n-1)^3} \left(\frac{\widehat{\text{Cov}}(X^2, Y)}{\widehat{\mu}_Y \widehat{\mu}_X^2} + \frac{4 \widehat{\text{Cov}}(X, Y)(\widehat{\text{Var}}(X) + \widehat{\mu}_X^2)}{\widehat{\mu}_Y \widehat{\mu}_X^3} \right) \\ &+ \frac{(n-2)(n-3)(n-4)(n-5)}{n^2(n-1)^2} \left(\frac{12}{n} r_a^* + \frac{30}{n(n-1)} \frac{\widehat{\text{Cov}}(X, Y)^2}{\widehat{\mu}_X^2 \widehat{\mu}_Y^2} \right) \end{aligned} \quad (124)$$

D.6 Term (f)

Term (f) is:

$$\frac{\text{Cov}(\bar{X}_2^3, \bar{X}_2)}{\mu_X^8} \quad (125)$$

The procedure to obtain its correction is analogous to that of term (e), hence we only present the result:

$$\begin{aligned} \frac{\text{Cov}(\widehat{X}_2^3, \widehat{X}_2)}{\widehat{\mu}_X^8} &= \frac{24(n-2)(n-3)(n-4)}{n^2(n-1)^3} \left(\frac{\text{Cov}(\widehat{X}^2, X)}{\widehat{\mu}_X^3} + \frac{4\widehat{\text{Var}}(X)(\widehat{\text{Var}}(X) + \widehat{\mu}_X^2)}{\widehat{\mu}_X^4} \right) \\ &+ \frac{(n-2)(n-3)(n-4)(n-5)}{n^2(n-1)^2} \left(\frac{12}{n} r_b^* + \frac{30}{n(n-1)} \frac{\widehat{\text{Var}}(X)^2}{\widehat{\mu}_X^4} \right) \end{aligned} \quad (126)$$

E Top-label calibration

Following standard practice in related work on calibration, we report the L_1 ECE^{bin} for top-label (also called confidence) calibration on CIFAR-10/100. ECE^{bin} was calculated using 15 bins and an adaptive width binning scheme, which determines the bin sizes so that an equal number of samples fall into each bin [Nguyen and O’Connor, 2015, Mukhoti et al., 2020]. The 95% confidence intervals for ECE^{bin} are obtained using 100 bootstrap samples as in Kumar et al. [2019]. In all experiments with calibration regularized training, the biased version of ECE^{KDE} was used.

Table 5 summarizes our evaluation of the efficacy of KDE-XE in lowering the calibration error over the baseline XE on CIFAR-10 and CIFAR-100. The best performing λ coefficient for KDE-XE is shown in the brackets. The results show that KDE-XE consistently reduces the calibration error, without dropping the accuracy. Figure 5 depicts the L_2 ECE^{bin} for several choices of the λ parameter for KDE-XE, using ResNet-110 (SD) on CIFAR-10/100. Figure 6 shows reliability diagrams with 10 bins for top-label calibration on CIFAR-100 using ResNet and Wide-ResNet. Compared to XE, we notice that KDE-XE lowers the overconfident predictions, and obtains better calibration than MMCE ($\lambda = 2$) and FL-53 on average, as summarized by the ECE value in the gray box.

Table 5: Top-label L_1 adaptive-width ECE^{bin} and accuracy for XE and KDE-XE for various architectures on CIFAR-10/100. Best ECE values are marked in bold. The value in the brackets represent the value of the λ parameter.

Dataset	Model	ECE^{bin}		Accuracy	
		XE	KDE-XE	XE	KDE-XE
CIFAR-10	ResNet-110	3.890 \pm 0.602	3.093 \pm 0.604 (0.001)	0.925 \pm 0.005	0.930 \pm 0.005
	ResNet-110 (SD)	3.555 \pm 0.623	2.778 \pm 0.468 (0.01)	0.926 \pm 0.005	0.932 \pm 0.005
CIFAR-100	ResNet-110	12.769 \pm 0.784	8.969 \pm 1.047 (0.2)	0.700 \pm 0.009	0.696 \pm 0.009
	ResNet-110 (SD)	11.175 \pm 0.642	7.828 \pm 0.814 (0.001)	0.728 \pm 0.009	0.721 \pm 0.009
	Wide-ResNet-28-10	7.279 \pm 0.876	3.703 \pm 1.086 (0.5)	0.762 \pm 0.008	0.770 \pm 0.008
	DenseNet-40	9.196 \pm 0.881	8.016 \pm 1.079 (0.01)	0.756 \pm 0.008	0.756 \pm 0.008

F Relationship between ECE^{bin} and ECE^{KDE}

In the following two sections, we investigate further the relationship between ECE^{bin} , as the most widely used metric, and our ECE^{KDE} estimator. For the three types of calibration, ECE^{bin} is calculated with equal-width binning scheme. The values for the bandwidth in ECE^{KDE} and the number of bins per class for ECE^{bin} are chosen with leave-one-out maximum likelihood procedure and Doane’s formula [Doane, 1976], respectively.

Figure 7 shows an example of ECE^{bin} in a three-class setting on CIFAR-10. The points are mostly concentrated at the edges of the histogram, as can be seen from Figure 7b. The surface of the corresponding Dirichlet KDE is given in 7c.

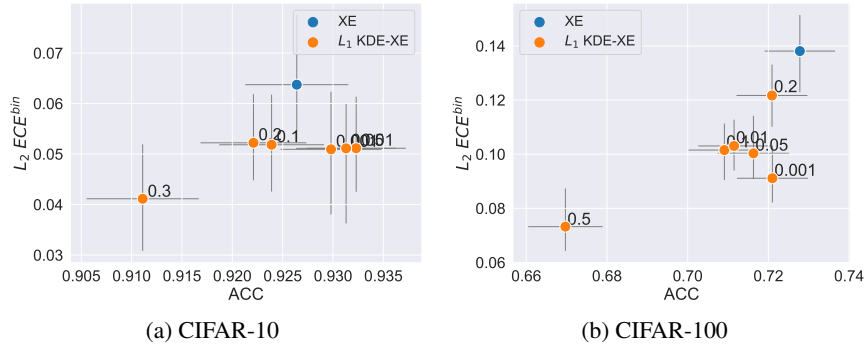


Figure 5: $L_2 ECE^{bin}$ for top-label calibration using ResNet (SD).

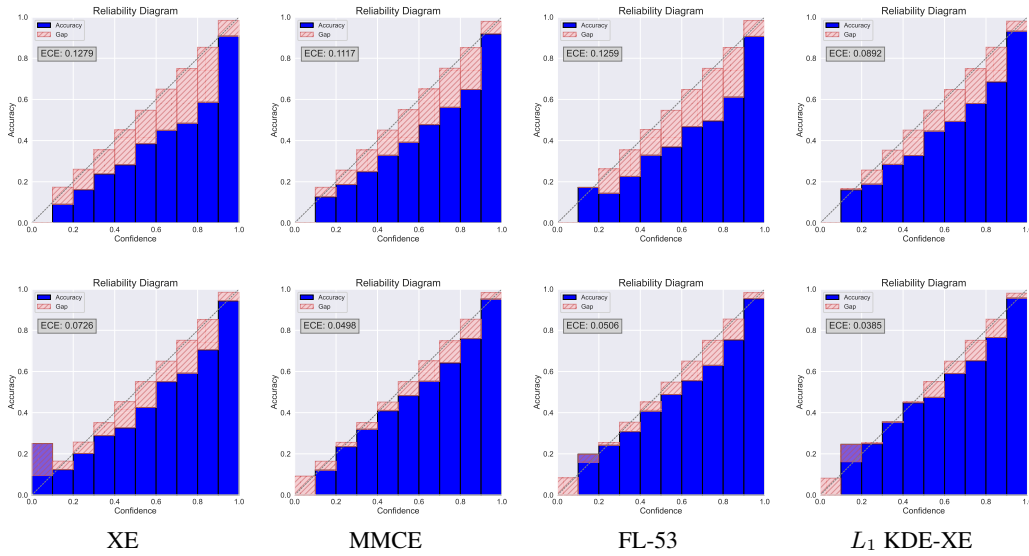


Figure 6: Reliability diagrams for top-label calibration on CIFAR-100 using ResNet (top row) and Wide-ResNet (bottom row) for each of the considered baselines.

Figure 8 shows the relationship between ECE^{bin} and ECE^{KDE} . The points represent a trained Resnet-56 model on a subset of three classes from CIFAR-10. In every row, a different number of points was used to estimate the ECE^{KDE} . We notice the ECE^{KDE} estimates of the three types of calibration closely correspond to their histogram-based approximations.

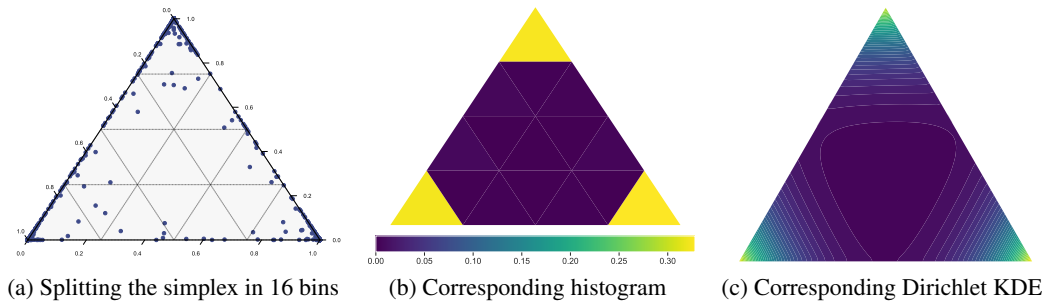


Figure 7: An example of a simplex binned estimator and kernel-density estimator for CIFAR-10

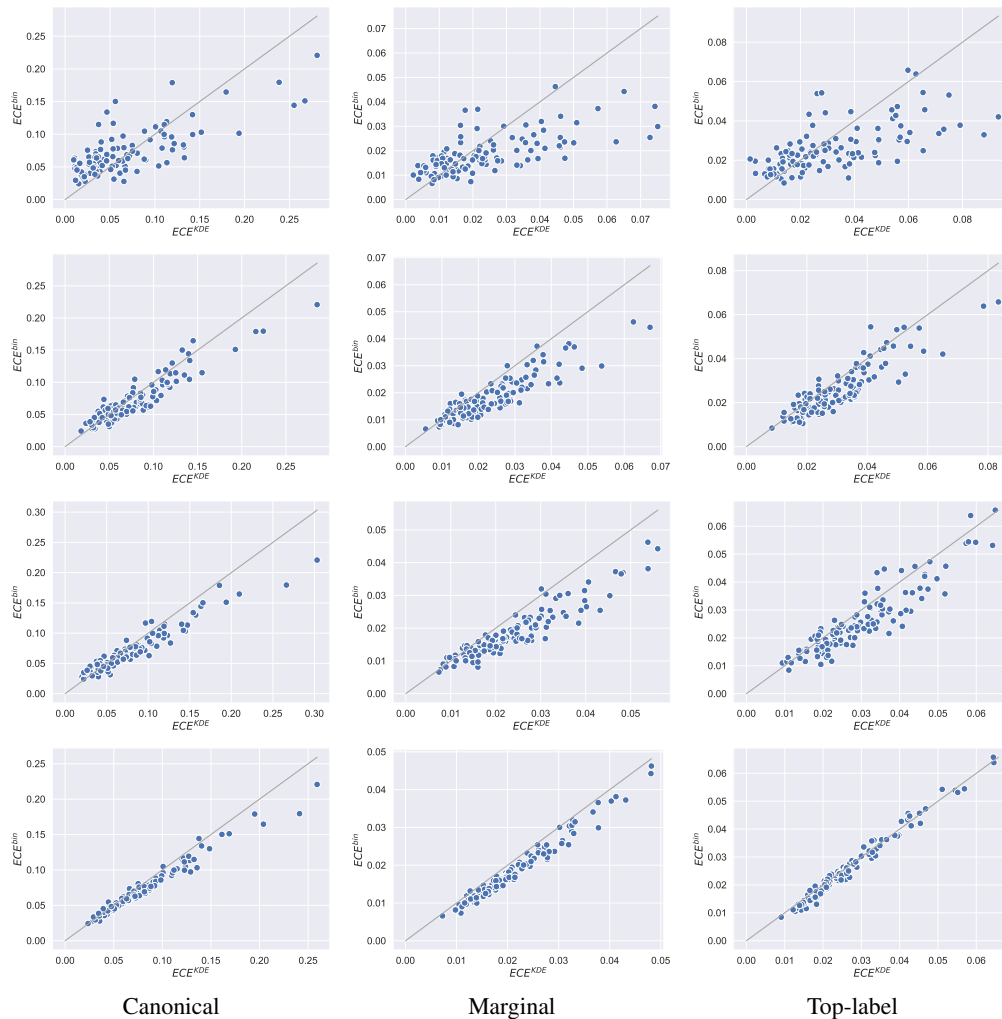


Figure 8: Relationship between ECE^{bin} and ECE^{KDE} for the three types of calibration: canonical (first column), marginal (second column) and top-label (third column). In every row top to bottom, different number of points (100, 500, 1000 and all points, respectively) are used to approximate ECE^{KDE} . Each point represents a ResNet-56 model trained on a subset of three classes from CIFAR-10. The number of bins per class (13) is selected using Doane’s formula [Doane, 1976], while the bandwidth is selected using a leave-one-out maximum likelihood procedure (typical chosen values are 0.001 for 100 points and 0.0001 otherwise).

G Bias and convergence rates

Figure 9 shows a comparison of ECE^{KDE} and ECE^{bin} estimated with a varying number of points. The ground truth is computed from 3000 test points with ECE^{KDE} . The used model is a ResNet-56, trained on a subset of three classes from CIFAR-10. The figure shows that the two estimates are comparable and both are doing a reasonable job in a three-class setting.

Figure 10 shows the absolute difference between the ground truth and estimated ECE using ECE^{KDE} and a ECE^{bin} with varying number of points. The results are averaged over 120 ResNet-56 models trained on a subset of three classes from CIFAR-10. Both estimators are biased and have some variance, and the plot shows that the combination of the two is in the same order of magnitude. The empirical convergence rates (slope of the log-log plot) is given in the legend and is shown to be close to the theoretically expected value of -0.5. We observe that ECE^{KDE} has similar statistical properties in terms of bias and convergence as ECE^{bin} .

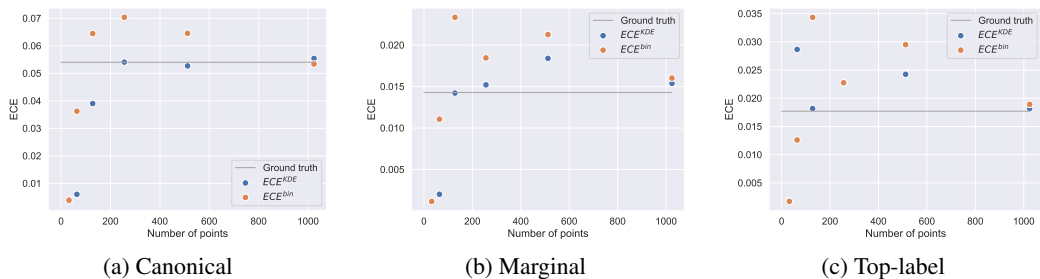


Figure 9: ECE^{KDE} estimates and their corresponding binned approximations on the three types of calibration for varying number of points used for the estimation. The ground truth is calculated using 3000 probability scores of the test set using ECE^{KDE} . Optimal number of bins and bandwidth are chosen with Doane’s formula and LOO MLE, respectively. Typical chosen number of bins is 6-11, and common values for the bandwidth are 0.0001 and 0.001.

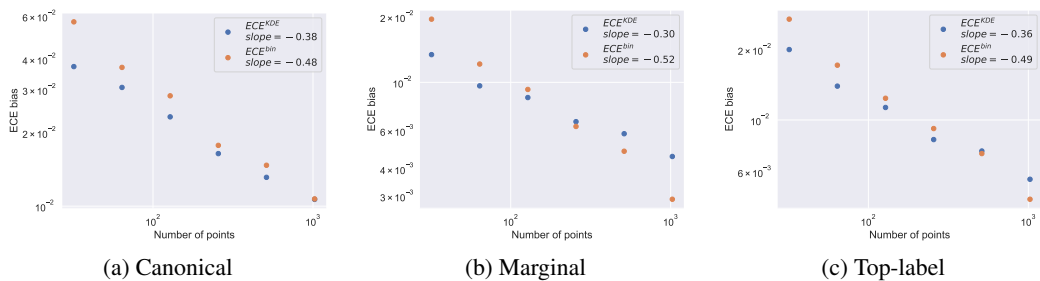


Figure 10: Absolute difference between ground truth and estimated ECE for varying number of points used for the estimation. The ground truth is calculated using 3000 probability scores of the test set. Note that the axes are on a log scale.